

# Ferroelectric

## 26. Ferroelectric Materials

Roger Whatmore

Ferroelectric materials offer a wide range of useful properties. These include ferroelectric hysteresis (used in nonvolatile memories), high permittivities (used in capacitors), high piezoelectric effects (used in sensors, actuators and resonant wave devices such as radio-frequency filters), high pyroelectric coefficients (used in infra-red detectors), strong electro-optic effects (used in optical switches) and anomalous temperature coefficients of resistivity (used in electric-motor overload-protection circuits). In addition, ferroelectrics can be made in a wide variety of forms, including ceramics, single crystals, polymers and thin films – increasing their exploitability. This chapter gives an account of the basic theories behind the ferroelectric effect and the main ferroelectric material classes, discussing how their properties are related to their composition and the different ways they are made. Finally, it reviews the major applications for this class of materials, relating the ways in which their key functional properties affect those of the devices in which they are exploited.

26.1	<b>Definitions and Background</b> .....	589
26.1.1	Basic Ferroelectric Characteristics and Models .....	591
26.2	<b>Ferroelectric Materials</b> .....	593
26.2.1	Ferroelectric Oxides .....	593
26.2.2	Triglycine Sulphate (TGS) .....	598
26.2.3	Polymeric Ferroelectrics .....	599
26.3	<b>Ferroelectric Materials Fabrication Technology</b> .....	600
26.3.1	Single Crystals .....	600
26.3.2	Ceramics .....	601
26.3.3	Thick Films .....	604
26.3.4	Thin Films .....	605
26.4	<b>Ferroelectric Applications</b> .....	607
26.4.1	Dielectrics .....	607
26.4.2	Computer Memories .....	607
26.4.3	Piezoelectrics .....	608
26.4.4	Pyroelectrics .....	611
	<b>References</b> .....	613

### 26.1 Definitions and Background

Ferroelectric materials offer a very wide range of useful properties for the electronic engineer to exploit. As we will see, they are also a class of materials that is hard to define accurately in a single sentence. It is useful to start from the class of insulating materials that form dielectrics; in other words materials that will sustain a dielectric polarisation under the application of an electric field. There exists a set of these materials for which the crystal structure lacks a centre of symmetry. (If a crystal structure has a centre of symmetry, it means that for every atom in the structure there is a point in the unit cell through which inversion will bring one to the same type of atom.) A list of the non-centrosymmetric, or *acentric*, point groups is given in Table 26.1. All of the crystalline materials whose structures possess these point groups (with the exception of group 432) exhibit the phenomenon

of piezoelectricity, which means that stress will generate a charge separation on the faces of the crystal (the direct piezoelectric effect) and will undergo mechanical strain when subjected to an electric field (the converse piezoelectric effect). Both effects are widely exploited in electronic devices. A well-known example of a non-centrosymmetric material is the mineral  $\alpha$ -quartz, which is used for the piezoelectric resonators employed for frequency filtering and electronic clocks.

A sub-set of the non-centrosymmetric crystals also possess a unique axis of symmetry. These crystals are said to be *polar*. The polar point groups are also listed in Table 26.1. Polar crystals are piezoelectric (as they are acentric) and also exhibit pyroelectricity, which means that a charge separation will appear on their surfaces when their temperature is changed. Polar structures effectively have a dielectric polarisation *built in* to the unit

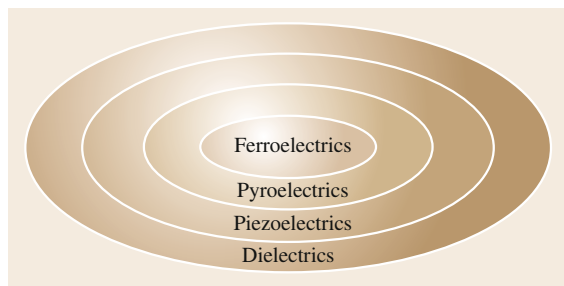
**Table 26.1** Polar and acentric (non-centrosymmetric) point groups

Crystal system	Polar (acentric)	Nonpolar (acentric)
Triclinic	1	
Monoclinic	2, $m$	
Orthorhombic	$mm2$	222
Trigonal	3, $3m$	32
Hexagonal	6, $6mm$	$\bar{6}$ , $\bar{6}m2$
Tetragonal	4, $4mm$	$\bar{4}$ , 422, $\bar{4}2m$
Cubic	None	23, $\bar{4}3m$ , 432

cell of the crystal structure. This is sometimes called a *spontaneous polarisation*. The application of stress or a change in temperature causes a change in this dipole moment and it is this change that causes the separation of charge on the surfaces of the crystal. The direction and magnitude of the spontaneous polarisation in a polar dielectric can be changed by the application of an electric field, but on removal of the field it will return to its zero-field value. A well-known example of a polar dielectric is ZnO, which possesses the wurtzite crystal structure in which  $Zn^{2+}$  ions sit in the tetrahedrally coordinated sites between hexagonal close-packed layers of oxygen ions. Thin films of ZnO are widely used for piezoelectric applications.

A sub-set of the set of polar dielectrics exists for which the application of a field of sufficient magnitude will cause the spontaneous polarisation to switch to a different, stable direction. Upon removal of the field the polarisation will not spontaneously return to its original direction and magnitude. These crystals are called *ferroelectric*. We can view the relationships between the sets of ferroelectric, polar, acentric and centrosymmetric dielectrics as shown in the Venn diagram in Fig. 26.1.

The history of ferroelectrics is long, as has been described in the excellent review by Busch [26.1]. Many very distinguished scientists were involved in its early development, including Brewster (who was one of those who studied pyroelectricity), J. & P. Curie (who discov-

**Fig. 26.1** Venn diagram showing how ferroelectrics fit into the different classes of dielectric materials

ered piezoelectricity), Boltzmann, Pockels and Debye, to name but a few. Indeed, the term ferroelectricity was first coined by E. Schrodinger. However, credit for the discovery of the effect goes to Joesph Valasek, who found in 1920 that the polarisation of sodium potassium tartrate (Rochelle salt) could be switched by the application of an electric field, thus providing the first demonstration of the process that is the hallmark of ferroelectricity.

A reasonable working definition of ferroelectricity is a *polar dielectric in which the polarisation can be switched between two or more stable states by the application of an electric field*. However, as we will see in the discussion which follows, there are exceptions to this definition: some ferroelectrics are semiconducting (and thus are not dielectrics because they cannot sustain an electrical polarisation); the spontaneous polarisation in some ferroelectrics cannot be switched because they cannot sustain an electric field of sufficient magnitude to effect the switching, either because they reach electrical breakdown first, or because they are too conducting.

Since the initial discovery of ferroelectricity in Rochelle salt, the effect has been demonstrated in a wide range of materials, from water-soluble crystals through oxides to polymers, ceramics and even liquid crystals. Many of these will be discussed in this chapter. The range of useful properties exhibited by ferroelectrics covers:

- Ferroelectric hysteresis is used in nonvolatile computer information storage.
- Ferroelectrics can exhibit very high relative permittivities (several thousand) which means that they are widely used in capacitors.
- The direct piezoelectric effect (the generation of charge in response to an applied stress) is widely used in sensors such as accelerometers, microphones, hydrophones etc.
- The converse piezoelectric effect (the generation of strain in response to an applied electric field) is widely used in actuators, ultrasonic generators, resonators, filters etc.
- The pyroelectric effect (the generation of charge in response to a change in material temperature) is widely used in uncooled infra-red detectors.
- The electro-optic effect (a change in birefringence in response to an applied electric field) is used in laser Q-switches, optical shutters and integrated optical (photonic) devices.
- Ferroelectrics exhibit strong nonlinear optical effects that can be used for laser frequency doubling and optical mixing.
- Illumination of transparent ferroelectrics with light of sufficient energy causes excitation of carriers into

the conduction band. Their movement under the internal bias field caused by the spontaneous polarisation causes a refractive-index modulation that can be used for a variety of optical applications, including four-wave mixing and holographic information storage.

- Ferroelectrics exhibit strong coupling between stress and birefringence, which can be used to couple acoustic waves to optical signals with applications in, for example, radar signal processing.
- Doping certain ferroelectric ceramics with electron donors (e.g., BaTiO<sub>3</sub> with La<sup>3+</sup>) can render them semiconducting. Heating these ceramics through their Curie temperature causes a very large, reversible increase in resistivity (by several orders of magnitude in some cases) over a narrow range of temperature (ca. 10 °C). This large positive temperature coefficient of resistance (PTCR) is widely exploited in electric-motor overload-protection devices and self-stabilising ceramic heating elements.

### 26.1.1 Basic Ferroelectric Characteristics and Models

The switchable spontaneous polarisation in ferroelectrics gives rise to the first characteristic property of the materials: ferroelectric hysteresis. Figure 26.2 shows a schematic plot of polarisation versus electric field as would be observed on a typical ferroelectric. As the field is increased from zero, the overall polarisation in the crystal increases as the polarisations in different dipolar regions are aligned. Eventually, it reaches a saturation point where the only further increase in  $P$  is that due to the relative permittivity of the material. (The gradient of the  $P/E$  curve for a linear dielectric is equal to its permittivity). Extrapolation of this line back to the abscissa gives the saturation value of the

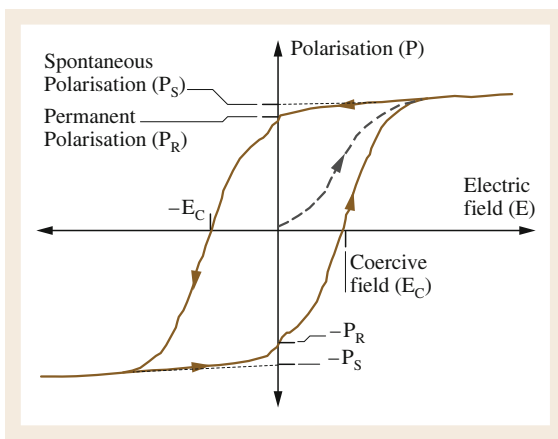


Fig. 26.2 Ferroelectric hysteresis loop

spontaneous polarisation ( $P_s$ ). Reduction of the field to zero leaves a *remanent polarisation* ( $P_r$ ), which is usually slightly less than  $P_s$ . A negative field will cause the polarisation to reduce, until it reaches zero at the *coercive field* ( $-E_c$ ). A further negative increase in the field will eventually cause a reverse saturation polarisation ( $-P_s$ ) to develop. When the field returns to zero the crystal is left with a negative remanent polarisation ( $-P_r$ ). Increasing the field once more increases the polarisation from  $-P_r$  to zero at  $E_c$ , and then to  $+P_s$ , completing the ferroelectric hysteresis loop. The ability to switch the polarisation between two states gives rise to the first application of ferroelectrics – as a nonvolatile memory storage medium. It also permits polycrystalline ferroelectrics (especially ceramics) to be polarised. The fact that the polarisation can possess different directions within different regions of the same crystal gives rise to the existence of *ferroelectric domains*. These are given names according to the angle between the polarisation between adjacent regions. Hence, two adjacent regions in which the polarisations are orientated at 180° to each other are, naturally, called 180° domains. In many ferroelectrics, the polarisation can choose between many different possible directions so that adjacent regions can have polarisations at, for example, 90° to one another.

For most ferroelectrics, the polar state only exists over a limited range of temperatures. As the temperature is raised, a point is reached at which there is a transition from the polar, ferroelectric phase to a nonpolar, non-ferroelectric phase (called the *paraelectric* phase). In all cases, the paraelectric phase possesses a higher crystal symmetry than the ferroelectric phase into which it transforms. The temperature at which this occurs is called the *Curie temperature* ( $T_C$ ). This ferroelectric-to-paraelectric phase transition is a characteristic of most ferroelectrics, but again there are exceptions. Some ferroelectric materials melt or decompose before  $T_C$  is reached; the polymeric ferroelectric polyvinylidene fluoride (PVDF) is one such example. For most ferroelectrics (called *proper ferroelectrics*), as the Curie temperature is approached from above, the relative permittivity is observed to increase, reaching a peak at  $T_C$  and decreasing below  $T_C$ . (There is a class of ferroelectrics, known as *improper* or *extrinsic ferroelectrics*, for which there is no peak in permittivity, just an anomaly. These are described further below.) Very high values of relative permittivity (many thousands) can be reached at  $T_C$ , leading to another use of ferroelectric materials – as dielectrics in high-value capacitors. The phase transition at  $T_C$  can either be continuous (known as second-order) or discontinuous (known as first-order). In either case, the dependence of permittivity ( $\epsilon$ ) on temperature above

$T_C$  can be described by  $\varepsilon = C/(T - T_0)$ .  $T_0$  is called the *Curie Weiss temperature*, and is only equal to  $T_C$  for a second-order phase transition.  $C$  is called the *Curie Weiss constant*. Figure 26.3 shows typical plots of  $P_s$  and  $\varepsilon$  as functions of temperature for ferroelectrics around  $T_C$ . Figs. 26.3a and 26.3b show the behaviour for a first-order phase transition. As can be seen,  $P_s$  drops discontinuously to zero at the phase-transition temperature. The permittivity rises as the temperature decreases, peaking at the transition, where there is a discontinuous step down. First-order phase transitions tend to show thermal hysteresis in the transitions, so that the transition occurs at a higher temperature when approached from the low-temperature side than from the high-temperature side. Frequently in practical observations there is actually a region of coexistence where both phases exist together in the same sample at the same temperature. In this case, the Curie temperature is defined as the temperature at which the ferroelectric and paraelectric phases have the same Gibbs free energies. In the case of a second-order phase transition (Figs. 26.3c and 26.3d),  $P_s$  drops continuously to zero at  $T_C$  and the permittivity rises to a sharp peak. There is no hysteresis in the transition.

There are two types of theoretical model that describe the ferroelectric phenomenon. The first is the phenomenological or thermodynamic theory first proposed by *Devonshire* [26.2]. Here, the Gibbs free energy of the ferroelectric system is described in terms of a power series in the spontaneous polarisation. In this

case,  $P_s$  is termed the order parameter for the phase transition and the theory is similar in form to the generalised phenomenological theory of phase transitions known as Landau theory. It is not appropriate to go into the details of the theory here, which has been described very well by *Lines and Glass* [26.3]. The theory successfully predicts many of the behavioural characteristics of ferroelectric materials in terms of the measurable macroscopic properties, including the ferroelectric hysteresis and the behaviour of the permittivity near  $T_C$ . However, it tells us nothing about the microscopic origins of ferroelectricity. This is the province of the two types of microscopic models of ferroelectric behaviour. The first of these is the order–disorder model of ferroelectric behaviour. The second is the displacive model.

According to the order–disorder model, the electric dipoles exist within the structure in the paraelectric phase above  $T_C$ , but are thermally disordered between two or more states so that the average polarisation is zero. There are several materials for which that is the case, an example being potassium dihydrogen phosphate (KDP), which is paraelectric, tetragonal ( $42m$ ) above 123 K and ferroelectric, orthorhombic ( $mm2$ ) below. The polarisation appears along the tetragonal  $c$ -axis. In this crystal structure, the  $PO_4$  groups form tetrahedra that are linked by hydrogen bonds at their corners. The protons in these sit in double potential wells. Above  $T_C$  they are delocalised between the two minima in the wells. Below  $T_C$ , they are localised and the  $PO_4$  tetrahedra become distorted. The phosphorous and potassium ions become displaced relative to the oxygen framework, forming the polarisation in the lattice. Replacement of the hydrogen in the structure by deuterium raises  $T_C$  to about 220 K because the heavier deuteron delocalises between the two potential minima at a much higher temperature. Another example of an order–disorder ferroelectric is sodium nitrite ( $NaNO_2$ ) in which the polar groups are  $NO_2^-$  ions, which become ordered below  $T_C$  (163 °C) with their dipoles all pointing along the  $b$ -axis of the crystal structure.

In displacive ferroelectrics, there are considered to be no dipoles in the structure above  $T_C$ , but the dipoles appear in the structure due to the cooperative motion of ions. Typically this is seen as the *softening* of a zone-centre optical phonon. What this means is that the frequency of an optical phonon mode with zero wavevector goes to zero at  $T_C$ . Such a phonon mode involves the displacement in opposite directions of cations and anions in the structure. When the frequency of this mode goes to zero, a dipolar displacement results. Examples of such ferroelectrics include the perovskite-structured oxides such as  $BaTiO_3$ , which will be discussed further below. One of the successes of soft-mode theory

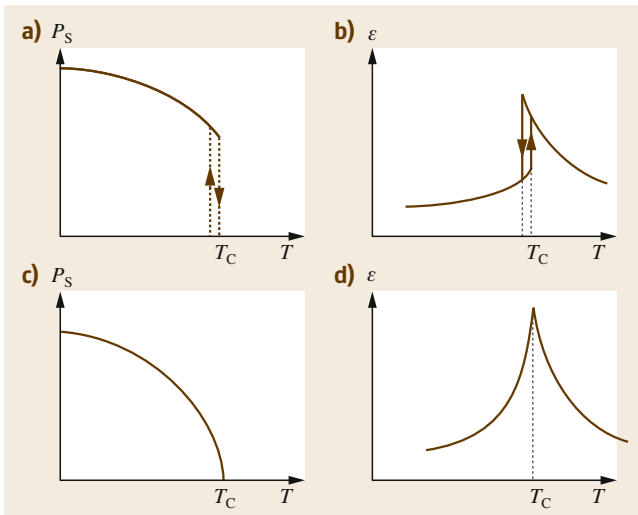


**Fig. 26.3a–d** The variations of spontaneous polarisation ((a) and (c)) and permittivity ((b) and (d)) with temperature for typical ferroelectric materials. (a) and (b) are for a first-order (discontinuous) phase transition while (c) and (d) are for a second-order (continuous) phase transition

is that it provides a convincing mechanism for the peak in the dielectric permittivity at  $T_C$ . According to the Lyddane–Sachs–Teller relationship (see, for example, [26.3] p. 216), the softening of a zone-centre phonon will make the permittivity diverge at  $T_C$ .

In practice, the distinction between order–disorder and displacive ferroelectrics becomes rather

blurred, as some ferroelectrics which may be considered to be purely displacive may exhibit significant disordered cation displacement well above  $T_C$ , while some order–disorder ferroelectrics show soft-mode behaviour. For a more detailed discussion of these theories, the reader is referred to *Lines and Glass* [26.3].

## 26.2 Ferroelectric Materials

### 26.2.1 Ferroelectric Oxides

This is by far the most technologically important class of ferroelectric materials. They will be discussed according to the most important crystal classes.

#### Perovskite Ferroelectrics

These materials possess crystal structures isomorphous with the mineral perovskite ( $\text{CaTiO}_3$ ). They all have the general chemical formula  $\text{ABO}_3$ , where A and B are cations. Typically the A cation will be around 1.2–1.6 Å in radius (similar to the oxygen ions) while the B cations will be around 0.6–0.7 Å in radius. The crystal structure is illustrated in Fig. 26.4. It consists of a network of corner-linked  $\text{BO}_6$  octahedra, within which is enclosed the large A cation. Another way to look at the structure is as cubic-close-packed  $\text{AO}_3$  layers, with the small B cations sitting in the octahedral sites between these close-packed layers. A pair of layers are shown in Fig. 26.5. The structure is a very tolerant one and will accommodate many different ions. Be-

cause of this, it is exhibited by a large number of oxides. The basic criteria for the structure to be stable is that the valencies of the ions should balance and that the ionic radii meet the *Goldschmidt criteria* [26.4]. A tolerance factor  $t$  is defined as

$$t = \frac{r_A + r_O}{\sqrt{2}(r_B + r_O)},$$

where  $r_X$  is the ionic radius of the X cation. The ideal cubic perovskite structure, where the ions are just touching each other, will possess  $t = 1$ . However, the structure will be stable with  $0.85 < t < 1.05$ . A list of ions that commonly form perovskites, together with their ionic radii, is given in Table 26.2. The closer  $t$  is to unity, the more likely the structure will be to be cubic. Conversely, perovskites which have values of  $t < 1$  show distorted structures that are frequently ferroelectric. Examples of some perovskites and their tolerance factors are listed in Table 26.3. This table also lists the structures formed by these compounds at

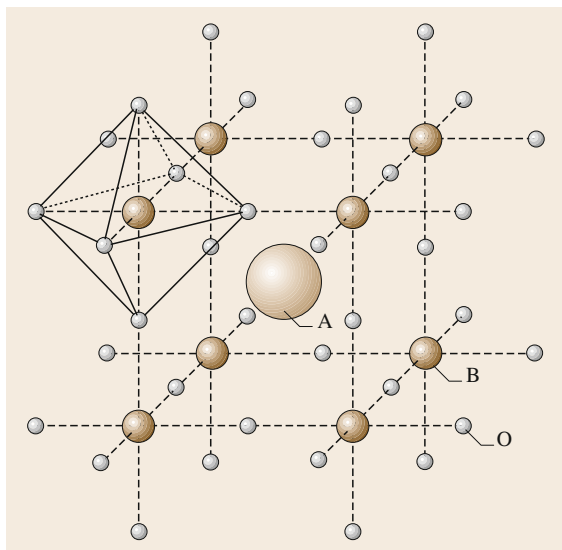


Fig. 26.4 The perovskite crystal structure

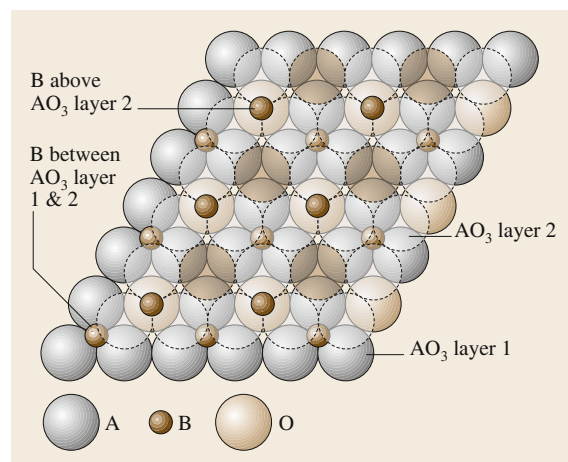


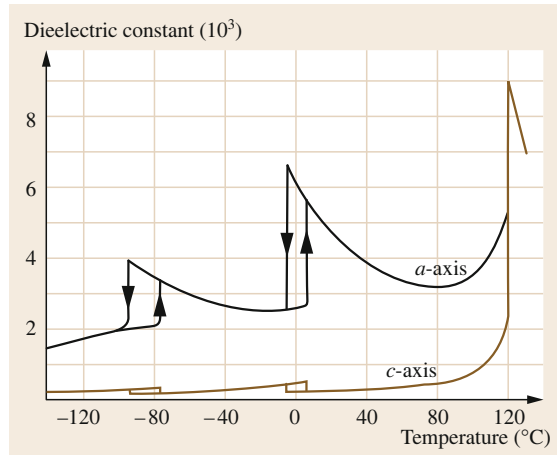
Fig. 26.5 Showing two  $\text{AO}_3$  close-packed layers of the perovskite structure, with the B cations sitting in the six-fold coordinated sites between the layers. The second layer has been made semitransparent for clarity

**Table 26.2** List of cations frequently found to form perovskite-structured oxides and their ionic radii. (Ionic radii taken from [26.5])

A-site cation	Ionic radius when [12] <sup>a</sup> by O <sup>2-</sup> (Å)	B-site cation	Ionic radius when [6] <sup>b</sup> by O <sup>2-</sup> (Å)
Na <sup>+</sup>	1.32	Nb <sup>5+</sup>	0.64
K <sup>+</sup>	1.6	Ta <sup>5+</sup>	0.68
Ba <sup>2+</sup>	1.6	Zr <sup>4+</sup>	0.72
Sr <sup>2+</sup>	1.44	Ti <sup>4+</sup>	0.605
Pb <sup>2+</sup>	1.49	Pb <sup>4+</sup>	0.775
Bi <sup>3+</sup>	1.11	Sc <sup>3+</sup>	0.73
Ca <sup>2+</sup>	1.35	Fe <sup>3+</sup>	0.645

<sup>a</sup> 12-fold coordinated; <sup>b</sup> 6-fold coordinated

room temperature, and whether or not they are ferroelectric. Some of the most interesting perovskites from the point of view of applications are BaTiO<sub>3</sub>, PbTiO<sub>3</sub> and KNbO<sub>3</sub>. BaTiO<sub>3</sub> is cubic above 135 °C, but transforms to a tetragonal ferroelectric structure below this temperature. In this case, the Ba and Ti ions are displaced relative to the anion framework along one of the cubic <001> directions. This means that the polar axis has six choices for direction in the tetragonal phase. At 5 °C there is a second-phase transition from the tetragonal to an orthorhombic phase, where the polarisation now appears due to cation displacements along one of the cubic <110> directions, for which there are 12 choices. Finally, at -90 °C there is a transition to a rhombohedral phase with the cations being displaced along one of the cubic <111> directions, for which there are eight choices. In the case of PbTiO<sub>3</sub> there is a single transition to a tetragonal phase at 490 °C, again by cationic displacements along <100>. Some perovskites show phase transitions that are not ferroelectric. For example, SrTiO<sub>3</sub> shows a transition to a tetragonal phase at 110 K which involves linked rotations, or tilts, of the TiO<sub>6</sub> octahedra about the cubic [100] direction. Tilting of the octahedra is a common feature of the phase transitions that occur in perovskites and can lead to very

**Fig. 26.6** Temperature dependence of the relative permittivity of BaTiO<sub>3</sub> measured along [001] and [100] (After [26.7])

complex series of phase transitions, as has been observed for NaNbO<sub>3</sub>. This type of structural modification and a commonly-used notation for it has been described in detail by Glazer [26.6].

It is very easy to make solid solutions of the end-member perovskites, such as those listed in Table 26.3, and this has been used to great effect to provide materials with a wide range of properties. For example, Fig. 26.6 shows the temperature dependence of the relative permittivity of a BaTiO<sub>3</sub> single crystal [26.7]. There is a peak at each transition where the value perpendicular to the polar axis reaches several thousand, making the material interesting for use in capacitor dielectrics. However, the temperature variation in such a material would make it useless. The formation of ceramic solid solutions of BaTiO<sub>3</sub> with SrTiO<sub>3</sub>, CaTiO<sub>3</sub> or PbTiO<sub>3</sub> allows the temperature dependence of permittivity to be controlled so that useful specifications can be met with average permittivities of 2000 or more over a wide range of temperatures. Herbert [26.8] has discussed the details of these modifications and their

**Table 26.3** Some end-member perovskites and their properties

Perovskite oxide	Tolerance factor	Structure at 20 °C	Type	T <sub>C</sub> (°C)
BaTiO <sub>3</sub>	1.06	Tetragonal	Ferroelectric	135
SrTiO <sub>3</sub>	1.00	Cubic	Paraelectric	
CaTiO <sub>3</sub>	0.97	Tetragonal	Paraelectric	
PbTiO <sub>3</sub>	1.02	Tetragonal	Ferroelectric	490
PbZrO <sub>3</sub>	0.96	Orthorhombic	Antiferroelectric	235
NaNbO <sub>3</sub>	0.94	Monoclinic	Ferroelectric	-200
KNbO <sub>3</sub>	1.04	Tetragonal	Ferroelectric	412
KTaO <sub>3</sub>	1.02	Cubic	Ferroelectric	-260
BiScO <sub>3</sub>	0.83	Rhombohedral	Ferroelectric	370
BiFeO <sub>3</sub>	0.87	Tetragonal	Ferroelectric	850

effects on the  $\text{BaTiO}_3$  transition temperatures.  $\text{BaTiO}_3$ -based ceramics are widely used in ceramic capacitors and form the basis of an industry worth billions of dollars annually. They have also been used for piezoelectric ceramics, but are no longer so important in that field, as they have largely been displaced by ceramics in the  $\text{PbZrO}_3$ - $\text{PbTiO}_3$  system. Nevertheless, there is a renewed interest in  $\text{BaTiO}_3$ -based ceramics for lead-free piezoelectrics in response to the legislative drive to reduce lead in the environment.

The perovskite solid solution system between  $\text{PbZrO}_3$  and  $\text{PbTiO}_3$  is of great technological importance and is thus worth discussing in some detail. The phase diagram given in Fig. 26.7 shows several phases. Starting at  $\text{PbTiO}_3$ , the ferroelectric tetragonal ( $F_T$ ) phase persists well across the diagram, until the composition  $\text{Pb}(\text{Zr}_{0.53}\text{Ti}_{0.47})\text{O}_3$  is reached, where there is a transition to a ferroelectric, rhombohedral phase. The composition where this occurs is called the morphotropic phase boundary (MPB). The rhombohedral phase region splits into two. There is a high-temperature phase ( $F_{R(HT)}$ ) in which the cations are displaced along the cubic [111] direction. There is also a low-temperature ferroelectric rhombohedral ( $F_{R(LT)}$ ) phase in which the  $(\text{Zr}, \text{Ti})\text{O}_6$  octahedra are rotated about the [111] axis. This doubles the unit cell. Close to  $\text{PbZrO}_3$  (Fig. 26.7b) the room-temperature structure transforms to the antiferroelectric, orthorhombic ( $A_O$ ) structure. This is a complex structure in which the cations are displaced in double antiparallel rows along the cubic  $\langle 110 \rangle$  directions, coupled with octahedral tilts. A higher-temperature  $A_T$  phase, which is frequently shown when this phase diagram is cited in the literature, has been shown not to exist in pure solid solutions [26.9]. There is another, more modern, modification to this phase diagram. It has been shown by *Noheda et al.* [26.10] that a monoclinic phase exists at the MPB (Fig. 26.7c). The enormous technological and commercial importance of this system derives from the very high piezoelectric, pyroelectric and electro-optic coefficients that can be obtained from ceramic compositions in different parts of the phase diagram, particularly when the base composition is doped with selected ions. These are discussed in more detail below. This solid solution system is frequently referred to generically as *PZT* although, strictly, *PZT* was the brand name for a set of piezoelectric ceramic compositions manufactured by the Clevite Corporation.

There is another very important class of oxides, termed complex perovskites, where the A or, more commonly B, sites in the structure are occupied by ions of different valency in a fixed molar ratio. These are not solid solutions as they possess a fixed composition. Examples are  $\text{PbMg}_{1/3}\text{Nb}_{2/3}\text{O}_3$  (PMN),  $\text{PbSc}_{1/2}\text{Ta}_{1/2}\text{O}_3$

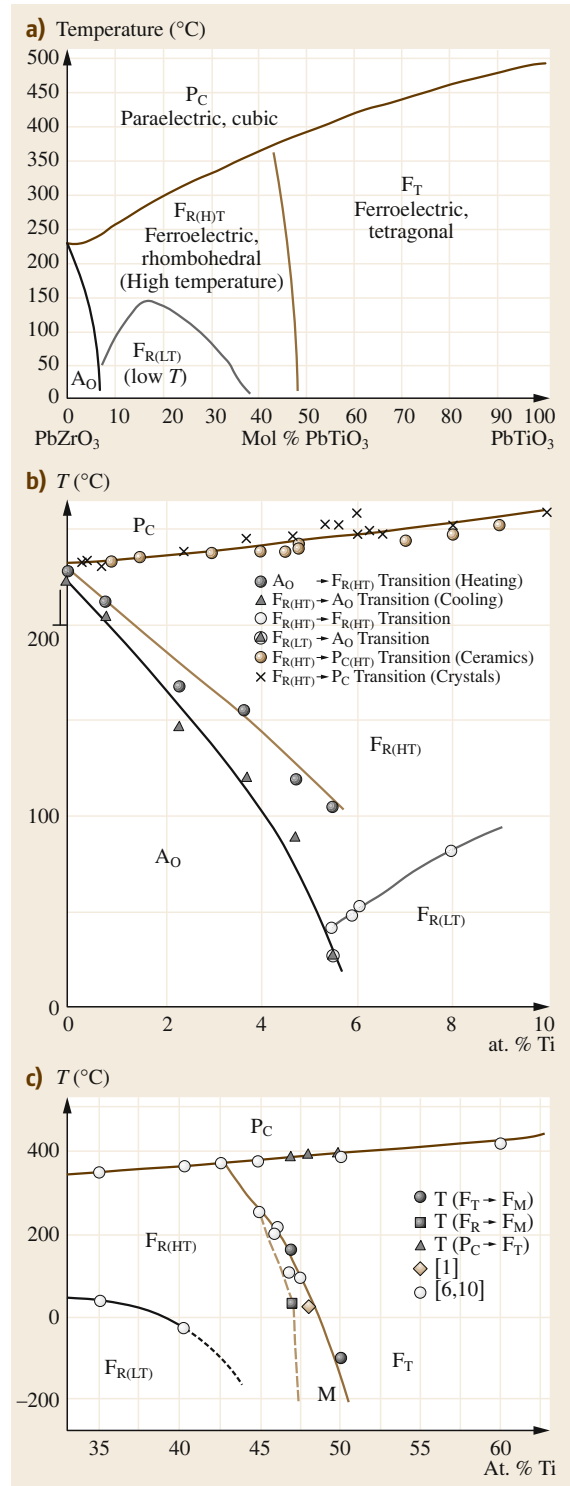


**Fig. 26.7** (a)  $\text{PbZrO}_3$ - $\text{PbTiO}_3$  phase diagram. (After [26.11]) (b) Region close to  $\text{PbZrO}_3$ . (After [26.9, 12]) (c) Region close to the MPB. (After [26.10])

(PST) and  $\text{Bi}_{1/2}\text{Na}_{1/2}\text{TiO}_3$ . These are also technologically important and can form end members to solid solutions in their own right,  $\text{PbMg}_{1/3}\text{Nb}_{2/3}\text{O}_3$ – $\text{PbTiO}_3$  (PMN-PT), for example. Many of the complex ferroelectrics (PMN-PT is a classic example) exhibit *ferroelectric relaxor* behaviour. In these materials, the Curie point is no longer a sharp transition but is actually observed over a very wide range of temperatures. A broad permittivity peak is observed and the temperature and height of the peak are strongly dependent on the frequency of measurement. Figure 26.8 shows a typical variation of permittivity with temperature and frequency in PMN [26.13].

The broad tolerance of the perovskite structure to different cations has led to a wide exploration of the inclusion of different iso-valent dopants to obtain different electronic properties. It is also possible to include alio-valent dopants over a wide range, which the structure tolerates through the introduction of cation or anion vacancies, or free charge carriers. For example, it is possible to incorporate  $\text{Nb}^{5+}$  into the B site of the  $\text{BaTiO}_3$  system [26.14], and charge balance is maintained through the presence of free electrons. Similarly,  $\text{Fe}^{3+}$  can be introduced into the B site of the system and this substitution creates O vacancies [26.15].

The vast majority of perovskites are employed in ceramic form, but thin- and thick-film materials are

becoming of increasing importance and single-crystal materials are starting to emerge which have exceptionally high piezoelectric coefficients.

### Ilmenite Ferroelectrics

The ilmenite structure is related to the perovskite structure in that it is exhibited by materials with the general formula  $\text{ABO}_3$ , where the A cation is too small to fill the [12] coordinated site of the perovskite structure. The structure is made up of hexagonal close-packed layers of oxygen ions, with the A and B ions occupying the octahedrally coordinated sites between the layers. Hence, this structure can also be considered to be related to the perovskite structure in that both are based on oxygen octahedra. The two best known ilmenite ferroelectrics are  $\text{LiNbO}_3$  and  $\text{LiTaO}_3$ , whose structure is shown in Fig. 26.9. The materials have high  $T_C$  values (ca. 1200 and 620 °C, respectively). In the case of  $\text{LiNbO}_3$ , the  $T_C$  is only 50 °C below the melting point. Referring to Fig. 26.9, it can be seen that the cations occupy octahedral sites progressing along the  $c$ -axis in the order Nb, vacancy, Li etc. The polarisation occurs through displacement of the cations along the three-fold axis, so the structure transforms from  $\bar{3}m$  to  $3m$  symmetry at  $T_C$ . These are *uniaxial* ferroelectrics, in that the polarisation can only be up or down, and only 180° domains exist. The materials are mainly used in

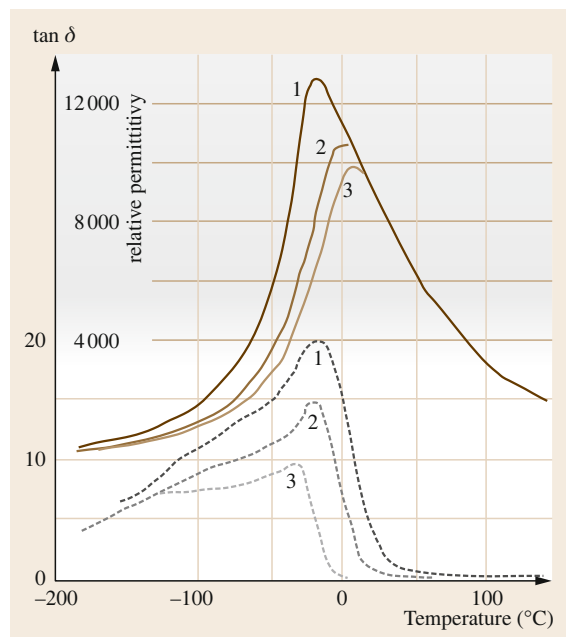


**Fig. 26.8** Permittivity (solid lines) and dielectric loss (dashed lines) versus temperature in PMN. The measurements were made at: (1) 0.4, (2) 45 and (3) 4500 kHz. (Adapted from [26.13])

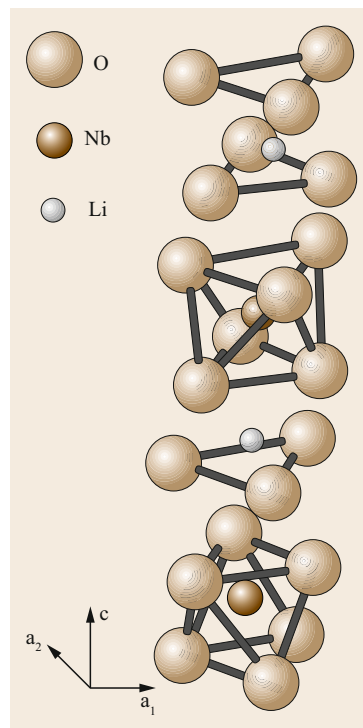


**Fig. 26.9** Crystal structure of  $\text{LiNbO}_3$ . (After [26.16])



single-crystal form for piezoelectric and electro-optic devices.

### Tungsten Bronze Ferroelectrics

This is another very large family of oxygen octahedral ferroelectrics possessing the general formula  $[A_1A_2A_4C_4][B_1B_2B_8]O_{30}$ . The crystal structure is complex, shown schematically in Fig. 26.10. The B1 and B2 sites are octahedrally coordinated by oxygens and have similar sizes and valencies to the B sites in the perovskites. The A1 and A2 sites are surrounded by four and five columns of  $BO_6$  octahedra respectively. The three-fold coordinated C sites in the structure are frequently empty, but can be occupied by small uni- or divalent cations (e.g.,  $Li^+$  or  $Mg^{2+}$ ). There are a wide range of ferroelectric tungsten bronzes, which frequently show nonstoichiometry. All are tetragonal in their paraelectric phase, and can transform to either a tetragonal ferroelectric phase, in which the polar axis appears along the tetrad axis of the paraelectric phase, or (more commonly) into an orthorhombic phase in which the polar axis appears perpendicular to the original tetrad axis. Examples of tungsten bronzes are  $PbNb_2O_6$  (lead metaniobate) in which five out of the available six A sites are occupied by  $Pb^{2+}$  and the B sites by  $Nb^{5+}$ . This crystal and its Ta analogue are metastable below about  $1200^\circ C$ . They can be stabilised by rapid cooling, or more commonly by doping. Lead metaniobate ceramics are difficult to make, but are commercially available and are occasion-

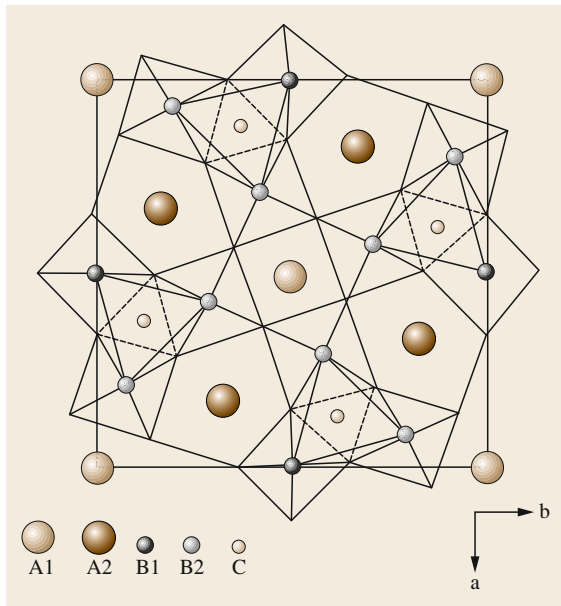
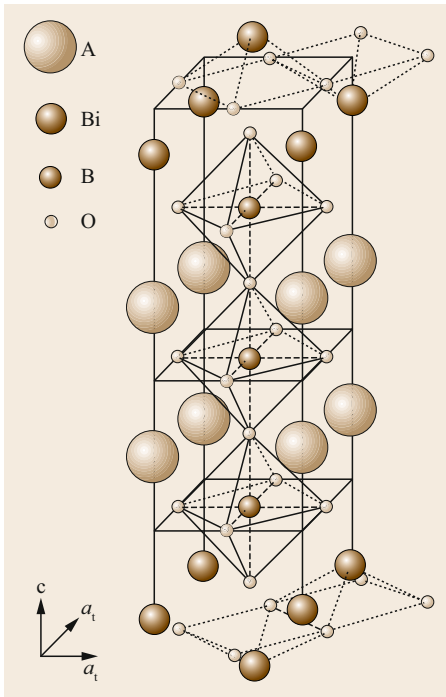


Fig. 26.10 Tungsten bronze crystal structure. (After [26.17])

ally used for piezoelectric devices by virtue of their higher Curie temperatures than members of the PZT system, combined with reduced lateral piezoelectric coupling factors. Substitution of  $Pb^{2+}$  by  $Ba^{2+}$  can also be used to produce a useful piezoelectric ceramic material  $Pb_{1/2}Ba_{1/2}Nb_2O_6$ . Other tungsten bronze ferroelectrics such as  $Sr_xBa_{1-x}Nb_2O_6$ ,  $Ba_2NaNb_5O_{15}$  and  $K_3LiNb_5O_{15}$  have been investigated as single crystals for use in electro-optic devices. However, the growth of highly homogeneous single crystals is difficult because of the formation of optical striations caused by compositional fluctuations.

### Aurivillius Compounds

The Aurivillius compounds form another important class of ferroelectrics based on oxygen octahedra. They have a good deal in common with the perovskites in that they consist of layers or slabs of perovskite blocks with the general formula  $(A_{m-1}B_mO_{3m+1})^{2-}$  separated by  $(M_2O_2)^{2+}$  layers in which the M cation is in pyramidal coordination with four oxygens, the M being at the apex of the pyramid. The structure possesses the general formula  $M_2(A_{m-1}B_mO_{3m+3})$ . In the ferroelectric phases, M is usually Bi and  $m$  is usually between one and five. The A and B cations follow the usual ionic radius and valency criteria of the perovskites, and we see ferroelectric compounds in which  $A = Bi, La, Sr, Ba, Na, K$  etc. and  $B = Fe, Ti, Nb, Ta$ , etc. Part of the crystal structure is shown schematically in Fig. 26.11, illustrating in this case a structure with  $m = 3$ . This is just over half of the unit cell, showing one slab of perovskite units and two of the  $(Bi_2O_2)^{2+}$  layers. The structures are tetragonal in their paraelectric phases, with the tetrad  $c$ -axis being perpendicular to the  $(Bi_2O_2)^{2+}$  plane. In the majority of cases they become orthorhombic in their ferroelectric phase, with the spontaneous polarisation appearing in the  $a-b$  plane, at  $45^\circ$  to the tetragonal  $a$ -axis. Bismuth titanate ( $Bi_4Ti_3O_{12}$ ) is an example of an Aurivillius ferroelectric in which  $M = A = Bi, B = Ti$  and  $m = 3$ , so that there are three blocks in the perovskite slab. In this case, there is a small component of the spontaneous polarisation (ca.  $4 \mu C/cm^2$ ) out of the  $a-b$  plane, with the majority of the polarisation (ca.  $50 \mu C/cm^2$ ) being in the plane, so that the ferroelectric structure is monoclinic. The  $T_C$  is high ( $675^\circ C$ ) and ceramics have been explored for use as high-temperature piezoelectrics. The problem with the compounds when used as ceramics is that the piezoelectric coefficients are rather small. Single crystals have been explored for optical light-valve applications but have not received widespread use because of the problems of growth. Thin films of  $SrBi_2Ta_2O_9$  (SBT) are receiving considerable attention for applications in ferroelectric nonvolatile memories. Recently, thin films of



**Fig. 26.11** Schematic diagram of half of the unit cell of the crystal structure of an Aurivillius compound with  $m = 3$ . The cell axes shown are those corresponding to the tetragonal structure

$\text{Bi}_6\text{Ti}_{2.8}\text{Fe}_{1.52}\text{M}_{10.68}\text{O}_{18}$  with  $m = 5$  have been shown to be single phase magnetoelectric multiferroics [26.18].

### Other Oxide Ferroelectrics

There is a wide range of other oxide ferroelectric materials, although none have anywhere near the breadth of application of the oxygen octahedral ferroelectrics discussed above. There are two groups of phosphates (in which the phosphorous ions are tetrahedrally coordinated by oxygens) which have found applications in optical systems. The potassium dihydrogen phosphate (KDP) family was referred to above as an example of an order–disorder ferroelectric. KDP, and its deuterated analogue  $\text{KD}^*\text{P}$ , can be grown from aqueous solution as large, high-quality single crystals. These can be lapped and polished into plates which are used for longitudinal electro-optic modulators, in which the modulating electric field is applied parallel to the direction of light propagation in the crystal. In this application, the crystals are used at room temperature in the paraelectric phase. One spectacular application for these crystals is as the Q-switches in the large ultra-high-power lasers used for nuclear fusion research, where extremely large (ca. 1 m) crystal slices are needed. Another class of phosphate ferroelectrics is the potassium titanyl phosphate (KTP) system. These crystals can be grown relatively easily from the melt and are used for optical frequency doubling applications, particularly using periodically poled crystals [26.19, 20]. This is a large family in which the

potassium can be replaced by caesium or rubidium and the phosphorous by arsenic. Lasers using KTP are finding significant uses in surgical procedures [26.21].

There are other examples of oxygen tetrahedral ferroelectrics. Lead germanate ( $\text{Pb}_5\text{Ge}_3\text{O}_{11}$ ) is an interesting material which has been prepared as a single crystal. It is a hexagonal uniaxial ferroelectric which is also optically active. Ge can be substituted up to 50% by Si, which reduces the Curie temperature from 177 to 60 °C. The sense of the optical rotation switches with the sign of the spontaneous polarisation. This has been considered for optical devices and pyroelectric infra-red detectors, but has not reached any commercial applications. It has been prepared in ceramic and thin-film form and is occasionally used as a sintering aid in lead-containing ferroelectric ceramics. Gadolinium molybdate,  $\text{Gd}_2(\text{MoO}_4)_3$  (GMO), possesses a structure consisting of corner-linked  $\text{MoO}_4$  tetrahedra. It is an example of an improper ferroelectric material in which the phase transition from the paraelectric phase is controlled by the softening of a zone boundary mode, which would lead to a nonpolar low-temperature phase, which is in fact *ferroelastic*. The high-temperature phase is acentric, and the ferroelastic lattice distortion couples via the piezoelectric coefficients to give a spontaneous polarisation. The lattice distortion can be reversed by electrically switching the spontaneous polarisation and vice versa. GMO has no commercial applications, although it was at one time considered for optical switches.

### 26.2.2 Triglycine Sulphate (TGS)

The TGS family is a salt of the simplest amino acid, glycine ( $\text{NH}_2\text{CH}_2\text{COOH}$ ) with sulphuric acid. In the crystal structure, the glycine groups are almost planar and pairs of them are connected by hydrogen bonds. A ferroelectric transition at 49.4 °C between two monoclinic phases is driven by an ordering of the protons in these hydrogen bonds. The replacement of these protons by deuterons (which can be accomplished by repeated crystallisation of TGS from heavy water) to give DTGS results in a 10 °C increase in  $T_C$ . There has been a great deal of academic interest in TGS because it possesses a well-behaved second-order order–disorder ferroelectric phase transition. In addition it has been of considerable technological interest for uncooled pyroelectric infra-red detectors and thermal imaging devices [26.22]. As a consequence, there has been considerable work on the replacement of various components with the objective of either improving performance or increasing  $T_C$ , such as can be achieved by deuteration. The replacement of glycine by l-alanine has been demonstrated to result in an internal bias field

in the crystal, which means that the crystals will retain their single-domain structure, even if heated well above  $T_C$ .

### 26.2.3 Polymeric Ferroelectrics

The first polymeric ferroelectric to be discovered was polyvinylidene fluoride (PVDF). The monomer for this possesses the formula  $\text{CH}_2\text{CF}_2$ . It was first shown to be piezoelectric by *Kawai* [26.23] and later *Bergman* et al. [26.24] speculated about the possibility of it being ferroelectric, although no Curie temperature could be shown to exist, as the polymer melts first. The structure of the polymer is complex, as the polymer backbone can adopt a number of configurations depending upon whether the neighbouring carbon-carbon linkages adopt trans or gauche configurations. In a trans (T) configuration, the groups bonded to the carbon atoms sit on opposite sides of the carbon-carbon bond. In a gauche (G) configuration, they sit on the same side. In an all-trans configuration, the carbon backbone of the polymer forms a simple zigzag. In the case of PVDF, there are four different phases with different T and G sequences, and with different ways the polymers stack together in crystal structures. The polymer crystallises from the melt into *form II*, also called the  $\alpha$ -phase, in which the bonds arrange themselves into the sequence TGT $\bar{G}$ , see Fig. 26.12. The fluorine atoms are strongly electronegative, which makes the C–F bond polar so that the molecule has a net dipole moment perpendicular to its length. However, the molecules of polymer arrange themselves in the unit cell so that the dipoles cancel each other out. Form II is neither ferroelectric nor piezoelectric, but application of an electric field will convert it into form II<sub>p</sub>, also called the  $\delta$ -phase, in which the polymer molecules are arranged so that the unit cell has a net dipole moment. High-temperature annealing of either of these forms will produce form III (the  $\gamma$ -phase), which has a new TGTTT $\bar{G}$ TT configuration which also has a net dipole moment perpendicular to the long axis of the molecule and these arrange in a crystal structure which is also polar. Subjecting forms II or III to stretching or drawing will produce form I (the  $\beta$ -phase), which is an all-trans configuration (Fig. 26.12). It can be seen from Fig. 26.12 that of the three molecular configurations, the polar bonds all point most-nearly in the same direction and this is retained in the unit cell. Electrical poling makes this the most-strongly piezoelectric phase of PVDF. The stretching

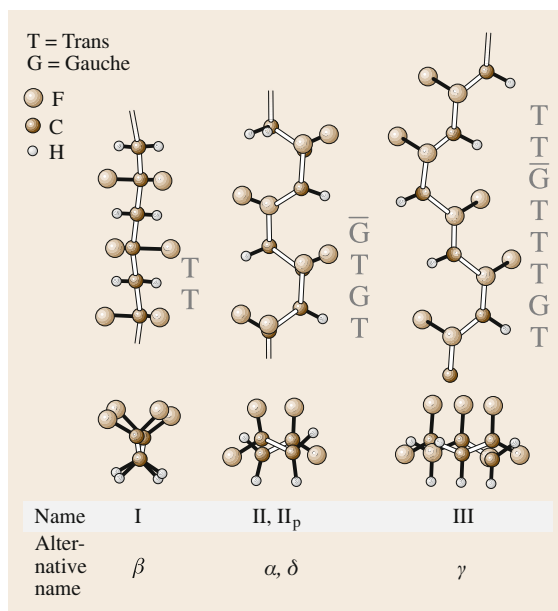


Fig. 26.12 PVDF bond structures

can be in a single direction, called uniaxial and usually achieved by drawing through rollers, or in two perpendicular directions, called biaxial and usually achieved by inflating a tube of polymer. Strong electric fields are needed for poling and these are frequently applied by placing the polymer under a corona discharge. The formation of a copolymer of vinylidene fluoride with between 10 and 46% trifluoroethylene (TrFE) leads to a polymer which will crystallise directly into form I (the  $\beta$ -phase) from either melt or solution. This can be poled to produce a material which is as active as pure PVDF. The copolymers also show clear signs of a ferroelectric-to-paraelectric transition, such as exhibiting peaks in permittivity at  $T_C$ , with a  $T_C$  that depends on the amount of TrFE in the copolymer. Extrapolation to 0% TrFE implies a  $T_C$  in PVDF of 196 °C. PVDF is readily available and has achieved moderately widespread use as a piezoelectric sensor material. It is particularly useful where light weight and flexibility are important, or where very large areas or long lengths are needed. The P(VDF-TrFE) copolymers are not as readily available and are not widely used. Other polymers that have been shown to exhibit ferroelectric behaviour include the odd-numbered nylons, but these are only weakly piezoelectric and have not achieved any technological uses.

## 26.3 Ferroelectric Materials Fabrication Technology

Ferroelectrics are used commercially in a very wide range of forms, from single crystals through polycrystalline ceramics and thin films to polymers. Hence, only a summary of the fabrication techniques can be presented here.

### 26.3.1 Single Crystals

As has been shown above, ferroelectrics often have a wide range of complex compositions. This renders the problems of single-crystal growth much more difficult than for single-element crystals such as silicon. In many cases, the most technologically useful compositions are themselves solid solutions of complex ferroelectric end members. Frequently these do not melt congruently and sometimes one or more components of the melt will be volatile. Some of the growth techniques which are used are:

#### Czochralski Growth

Certain ferroelectric crystals melt congruently and can be pulled from the melt using the Czochralski technique. Examples include  $\text{LiNbO}_3$  and  $\text{LiTaO}_3$ . Both materials are widely used technologically.  $\text{LiNbO}_3$  is used in surface acoustic wave (SAW) and electro-optic devices and  $\text{LiTaO}_3$  in pyroelectric infrared detectors, piezoelectric resonators, SAW and electro-optic devices.  $\text{LiNbO}_3$  melts congruently at  $1240^\circ\text{C}$ , but the congruently melting composition is not at the stoichiometric composition ( $\text{Li} : \text{Ta} = 1$ ), but lies at around 49%  $\text{Li}_2\text{O}$ . Crystals pulled from such melts in platinum crucibles are perfectly adequate for piezoelectric and most optical applications. However, it is known that the stoichiometric composition possesses rather better optical properties than the congruent composition and there is now a premium-grade material available commercially.  $\text{LiTaO}_3$  melts congruently at  $1650^\circ\text{C}$ . Again, the composition is not at  $\text{Li} : \text{Ta} = 1$ , but is slightly Ta deficient. The growth temperature is above the melting point for platinum. The solution is to use crucibles made from iridium, which is very expensive. Also,  $\text{IrO}_2$  is volatile so the growth atmosphere must be  $\text{N}_2$ , which means that the crystals come out of the melt oxygen-deficient and must be embedded in  $\text{LiTaO}_3$  powder and annealed under  $\text{O}_2$  after growth to make them clear. Pt/Rh crucibles have been used to grow  $\text{LiTaO}_3$  crystals, but the Rh absorbed into the crystals makes them brown. Such crystals are acceptable for piezoelectric and pyroelectric, but not for optical, applications. Virtually all ferroelectric materials need to be electrically poled before use. In the case of  $\text{LiTaO}_3$ , silver electrodes are applied to faces perpendicular to the polar

(c) axis and a pulsed field of about  $10\text{ V/cm}$  (1 ms with a 50/50 duty cycle) applied while the crystal is cooled slowly through  $T_C$  ( $620^\circ\text{C}$ ). A similar process can be applied to pole  $\text{LiNbO}_3$  crystals or, as the  $T_C$  is very close to the growth temperature, the field can be applied between the growing crystal and the crucible. This process has also been used to grow periodically poled crystals in which the field is reversed periodically during the growth of the crystal. Such crystals have some advantages in optical frequency-doubling in a process known as quasi-phase matching [26.25].

#### Solution and Flux Growth

The growth of crystals from aqueous solution is a technology very readily applied to water-soluble materials such as KDP and TGS. There are two processes that have been used. The first consists of rotating crystal seeds in a bath of saturated solution, which is slowly cooled so that material that comes out of solution is deposited on the seeds. The second consists of recirculating the bath solution over feed material, which is held at a slightly higher temperature and then back over the slightly cooler seeds, where the feed material is deposited. In both techniques, very careful control of temperature is essential (better than  $0.002^\circ\text{C}$ ) and the growth process can take many days.

The process of growing oxide single crystals from solution or flux is closely related to the above process, in that the crystals are grown from a saturated solution of the required oxide in a molten flux as it is slowly cooled. In the simplest version of this process, the oxides are sealed in a platinum crucible, heated to a *soak* temperature and slowly cooled to room temperature. Small crystals (usually up to a few mm in size) can then be recovered from the solidified melt. This has been applied to growth of a wide variety of small single crystals, such as PZT and PMN-PT solid solutions. PZT, for example, can be grown from  $\text{PbO}-\text{B}_2\text{O}_3$  flux mixtures, or even pure  $\text{PbO}$  [26.26].  $\text{BaTiO}_3$  crystals can be grown from  $\text{KF}$  or  $\text{TiO}_2$  fluxes. A major issue with the growth of Pb-containing ferroelectrics from  $\text{PbO}$  rich fluxes is the evaporation of  $\text{PbO}$  from the melt at the crystallisation temperature over the long time periods required to grow large crystals. This can be avoided to some degree by the use of sealed crucibles. A variation on the flux growth process is top-seeded solution growth, whereby a seed crystal is immersed from above into a supersaturated solution of the material to be grown. The crystal then grows as the solution is cooled further. The process is difficult to control and it has the major problem, especially when growing from a  $\text{PbO}$  flux, that the melt is open and therefore very prone to

flux evaporation. It has been successfully applied to the growth of crystals of PMN-PT and PZN-PT solid solutions. The Bridgman process seeks to get over this problem by placing a dense compact of the flux/solute mixture inside a sealed crucible with a conical end, as shown in Fig. 26.13. A seed crystal is placed at the base of the cone which is held cooler than the rest of the crucible by a cooled rod. A molten zone is then allowed to travel up the crucible and the crystal solidifies inside it. Good-quality crystals have been grown this way and it is the preferred technique for the manufacture of PMN-PT and PZN-PT solid solutions. One problem with all flux-growth techniques is that the flux composition is constantly changing during the growth process and therefore the crystals tend to be nonuniform in composition. This is a particular problem for larger crystals, especially for solid solutions.

### 26.3.2 Ceramics

The vast majority of ferroelectric materials that are used commercially are used in the form of polycrystalline ceramics. These are used in many of the applications listed above, including as dielectrics and in piezoelectric, pyroelectric, PTCR and electro-optic devices. Many different ferroelectric ceramic fabrication technologies have been developed over the years, but they are all based around a similar fabrication sequence. The

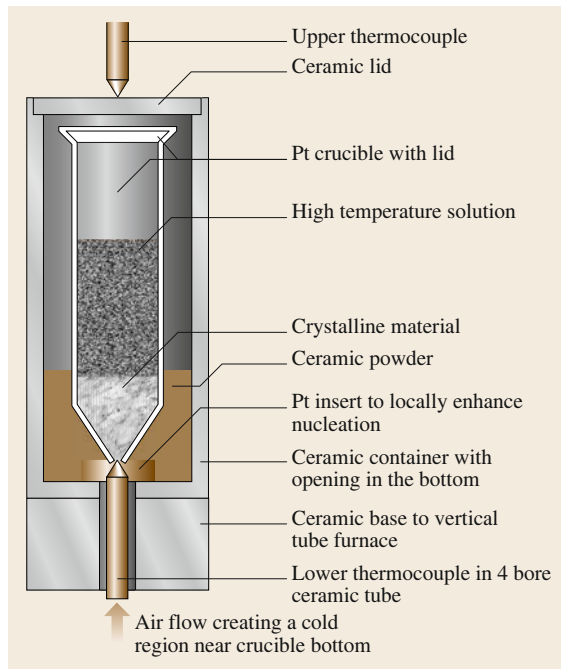


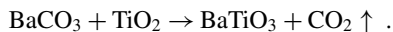
**Fig. 26.13** A modified Bridgman apparatus used for growing piezoelectric single crystals. (After [26.27])

key points are discussed below. Note that as the vast majority of commercially exploited ferroelectrics are oxides, the discussion will centre around these materials:

- **Raw-material selection:** The usual starting point for a ceramic fabrication sequence is the selection of the raw materials. For oxide ferroelectrics, the raw materials are usually oxides or carbonates, but occasionally other compounds (e.g. nitrates, citrates etc.) are used which will decompose when heated to form the oxides required. High purity (usually > 99.9% with respect to unwanted cations) is important for good reproducibility. Small quantities of dopants can have a major effect on the final electrical properties, as would be expected for any electronic material, but can also seriously affect the sintering characteristics and grain size of the final ceramic body. Note that high purity does not usually imply the kind of purity that would be needed for a semiconductor material. Indeed, ultra-high purity (> 99.99%) is often obtained by raw-material manufacturers by applying processes which negatively affect the reactivity of the oxide powders. A high degree of solid-state reactivity in the powders is important for the processes which follow. This is usually determined by a combination of raw-material particle size and specific surface area, although selecting the right crystallographic phase can be important. When using  $\text{TiO}_2$ , for example, it is usually found that the anatase phase is more reactive than rutile. These factors can be analysed for quality control purposes by using laser particle size analysis (taking care to break up loosely bound agglomerates by ultrasonic dispersion in water, with a dispersing agent prior to measurement), BET (Brunauer, Emmett and Teller)-specific gas absorption and x-ray powder diffraction respectively. The majority of ceramics are made by mixing together powdered raw materials, but occasionally solution mixing techniques are used and these will be discussed further below.
- **Raw-material mixing:** This is usually done in a ball mill consisting of a cylinder containing a mixture of small balls or cylinders made of steel, steatite, zircon or yttria-stabilised zirconia (YSZ). The oxide raw materials are accurately weighed into the ball mill, together with a predetermined amount of a milling fluid (usually deionised water, but occasionally an organic fluid such as acetone). It is usual to add a dispersant to aid the breakup of agglomerates. The ball mill is then sealed and rotated to mix the ingredients. Precise milling conditions are determined by the materials being used, but

the mixing time is usually of the order of a few hours. It is advantageous to use milling balls that are made of a material whose wear products will be reasonably innocuous in the final ceramic. For this reason, YSZ balls are preferred over steel or steatite, as small amounts of iron and silica contaminants can have unwanted or deleterious effects on the properties of many ferroelectric ceramics. For similar reasons, the ball mills are frequently rubber lined. Many variations on this process have been explored. High-energy ball milling is receiving considerable attention. In this process, the milling balls are given very high energy by either aggressively vibrating the ball mill or by stirring them at high speed with a paddle. Raw materials trapped between the balls are both comminuted and, if the energy is sufficiently high, can be forced to react together. Crystalline raw materials can be made amorphous in this process. A significant amount of energy can be stored in the powders after this process so that subsequent sintering can be undertaken at lower temperatures. In an adaptation of this process, it can be done in a continuous flow-through mill, whereby the slurry is pumped through the high-energy mill, making it less of a batch process.

- **Drying:** The slurry that results from the mixing process is dried after the milling balls are removed. On a small scale, this can be done in an oven or by freeze drying, but on a commercial scale, this is usually achieved by spray drying.
- **Calcination:** The purpose of this process is to react the raw materials into the required crystallographic phase. The dried powders are placed into a sealed crucible (usually high-purity alumina or zirconia), which is baked in a furnace at a temperature high enough to decompose any non-oxide precursors and cause a solid-state reaction between the raw materials, but not so high as to sinter the particles and form hard agglomerates that will be difficult to break up in subsequent processing. A simple example is the reaction between  $\text{BaCO}_3$  and  $\text{TiO}_2$  to form  $\text{BaTiO}_3$



This reaction will go to completion at about  $600^\circ\text{C}$ . Note that a much higher temperature ( $> 1000^\circ\text{C}$ ) is required for the decomposition of  $\text{BaCO}_3$  to  $\text{BaO}$  in the absence of  $\text{TiO}_2$ .

- **Milling:** This is usually done in a similar manner to the mixing process described above, but is done for longer. The objective is to break up hard agglomerates and reduce the powder to its primary particle size. Again, high-energy milling techniques can be used. Dispersants are usually added to aid the pro-

cess, and pH is controlled so that the powder does not flocculate. Organic binders can be added at this stage. The slurry from the milling process is usually spray-dried or freeze-dried as a free-flowing aggregated powder is required. The objective is to form soft aggregates that will break up on subsequent die pressing. Alternatively, the slurry (or *slip*) can be taken straight to a slip- or tape-casting process.

- **Shape forming:** After drying, the powders from the above process can be uniaxially pressed into the *green* shape required, typically using a steel punch and die-set. It is important in this process to make sure that the force is applied equally to top and bottom punches. Usually, the die is designed with a slight taper to ease removal of the workpiece after pressing. Faults that can occur at this stage of the process include *capping* or radial cracks in the work piece, which usually result from an uneven distribution of pressure. One way to avoid this is to use cold isostatic pressing. In this process the powder, or more frequently a lightly uniaxially cold-pressed green block, is vacuum-sealed into a rubber mould, which is then immersed in a bath of oil. The oil is taken up to a high pressure, which isostatically compresses the block. The advantage of using this process is that it avoids the nonuniform distribution of pressure that is frequently a problem with uniaxially cold pressing. The high pressure allows the agglomerates to be broken up and the process usually results in a much higher green density, which facilitates the sintering process. Another process that can be used to form the green item is slip-casting, which involves pouring the ceramic slip into a plaster mould, which is usually gently rotated. The plaster absorbs moisture from the slip and the ceramic particles are deposited as a layer. Surplus slip is poured off and the deposited layer can be separated from the mould after it is dry. This process has been used to make large cylinders of piezoelectric ceramics. A third process that is frequently used to make thin sheets of ceramic is tape-casting, by which the slip is passed under a set of *doctor blades* in the apparatus shown schematically in Fig. 26.14. In this case, the slip is cast onto a continuous roll of plastic tape and a plastic binder is added to the slip which, when dry, holds the powder together and makes a flexible green tape. Sometimes the slip is cast directly onto a glass sheet. The green tapes can be screen-printed with patterns of metallic electrode inks and then laminated by warm-pressing to make multilayer structures with interleaved electrodes. This type of fabrication is widely used for multilayer ceramic (MLC) capacitors and multilayer ceramic piezoelectric actuators.

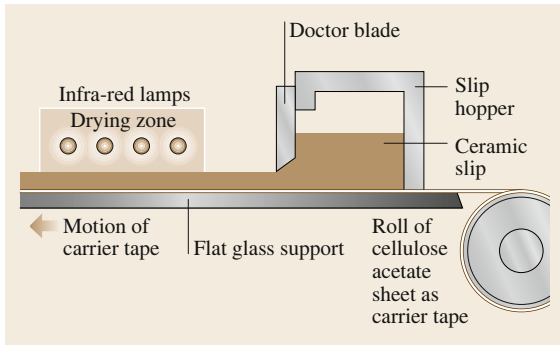


Fig. 26.14 Tape-casting apparatus

- **Sintering:** The green ceramic bodies are sintered in furnaces at temperatures of 1150–1300 °C, depending on the ceramic being manufactured. There is a good deal of process know-how in the sintering of the ceramic bodies. Key issues are:
  - The heating profile, which must be carefully controlled, especially over the lower range of temperatures up to about 500 °C where the organic matter (dispersants and binder) is burned off. Too rapid heating will cause large pores, or even cracks, to form.
  - For lead-containing ceramics, it is important that air be allowed free access to the vaporising organic material, or it will be carbonised and this can lead to reduction of the PbO in the ceramic to free Pb.
  - Loss of PbO by volatilisation at higher temperatures ( $> \approx 800$  °C) means that the ceramic body needs to be sintered in a PbO-rich environment, which is often produced by packing the ceramic body in a *spacer powder* of  $\text{PbZrO}_3$ , or PZT ceramic chips within well-sealed ceramic crucibles or saggars. This tends to restrict the access of air to the sintering ceramic body, which conflicts with the previous requirement.
  - The ceramic body must be free to move during the sintering process, as there is significant linear shrinkage (about 15 to 18%). If the body is unable to slide over the surface on which it sits, this can lead to cracking, especially for large components. One solution to this problem is to sit the body on zirconia sand.

The sintering process has been very well described elsewhere. It is possible to obtain very high densities ( $> 98\%$ ) by careful control of the sintering conditions. For Pb-containing ferroelectric ceramics, a small excess of PbO is usually added to compensate for PbO loss by evaporation. This also tends to act as a liquid-phase-sintering aid, lubricating the grains of ceramic as they slide over each other

in the sintering process, and providing a surface-tension force that pulls the ceramic grains together. The PbO also acts as a solvent, aiding the movement of the ceramic components during sintering and further densifying the ceramic. It is possible to sinter such materials to transparency, which means that there is virtually zero porosity. Very high densities can also be obtained by hot-pressing, in which the green body is placed inside a ceramic punch and die-set and raised to the sintering temperature under a pressure of about 35 MPa. Alternatively, hot isostatic pressing (HIP) can be used. In this process the pressure transmitting medium is a high-pressure gas (usually argon, but if the ceramic is Pb-containing it is important to include a few percent of oxygen to prevent reduction of the ceramic). In this case pressures of 100 MPa or more can be used. If the ceramic is pre-sintered so that there is no open porosity, then this can be achieved without the need for any container, but if there is open porosity, the body must be encapsulated in a suitable metal container, which will usually need to be a noble metal such as Pt.

- **Electroding:** Good-quality electroding is essential for all ferroelectric devices for a variety of reasons. Any low-permittivity layer between the electrode and the ferroelectric material will manifest itself in a fall-off in capacitance and an increase in loss as the frequency of measurement is increased. Poor-quality electrodes, or even the wrong type of conductive material can lead to problems with device ageing, or even an inability for the device to function as intended. Most piezoelectric materials are supplied with a *fired-on* silver electrode, which is a mixture of silver powder, a finely divided glass frit and a fluxing agent. Obtaining the correct balance between metal and glass contents is important, as too high a proportion of metal will lead to poor electrode adhesion while too high a proportion of glass will lead to poor electrode conductivity. Such electrodes are solderable with the use of appropriate fluxes. Sputtered or evaporated metal electrodes such as Ni or Cr/Au can also be used, as can metal electrodes deposited by electroless processes (e.g., Ni). The ohmic nature of the electrode contact to the ceramic is not usually important for highly insulating materials, such as piezoelectrics, but is important for semiconducting ceramics such as PTCR  $\text{BaTiO}_3$ . In this case it is usual to use Ni electrodes, which need to be annealed after deposition to develop the ohmic contact. In some cases it is necessary to fire on the electrode at the same time as ceramic sintering (cofired electrodes). This is particularly important

where the electrodes are buried in the structure, as with MLC capacitors and actuators. Clearly, there are problems to solve here in terms of the potential oxidation or melting of the electrode material. The conventional materials to use in such electrodes have been noble metals such as palladium (sometimes alloyed with silver) or platinum, which are very expensive. There have been serious efforts to develop ferroelectric compositions that can be fired with base metal electrodes such as Ni. In the case of BaTiO<sub>3</sub>-based dielectrics, this has entailed the development of heavily acceptor-doped compositions that can stand being fired in a neutral or slightly reducing atmosphere. In the case of MLC actuators, there has recently been some success in developing piezoelectric PZT compositions that can stand being fired in such atmospheres, using Cu as the electrode material.

- Poling: Many devices made from ferroelectric ceramics (all piezoelectric and pyroelectric devices) require poling before they will develop useful properties. This entails applying a field that is significantly in excess of the coercive field (typically 3×), usually at an elevated temperature. It is not usually necessary to exceed the Curie temperature. For example, PZT ceramics with  $T_C$  in the range 230–350 °C can be poled by applying 3–5 kV/cm (depending on the type of PZT – see below – soft PZTs need lower poling fields than hard PZTs) at about 150 °C, with the field kept applied while the workpiece is cooled to room temperature. It is usual to immerse the ceramic in a heated bath of oil (mineral or silicone) during the process. One disadvantage of this is that the ceramic then needs to be carefully cleaned after poling. Silicone oil can be very hard to remove completely and its presence as a residue will compromise electrode solderability. For this reason, some workers have developed a process whereby the ceramic is poled under SF<sub>6</sub> gas. There is a rapid decay of properties after poling. This decay stabilises after a few hours, so it usual to wait at least 24 hours before electrical properties are measured.

There are many variations on the above basic process route which have been researched. One of these is the use of solution techniques to prepare the oxide powders. The basic principle here is that if the cations are mixed in solution, then they will be mixed on the interatomic scale without the need for milling processes that can introduce impurities. (This is a matter of discussion, as the act of precipitation and decomposition can lead to separation of the components.) Many routes have been explored, including the use of inorganic pre-

cursors such as nitrates and metalorganic precursors such as oxalates, citrates or alkoxides and acetates. Some of these have achieved a degree of commercial success, although the use of solution routes is more complex and the raw materials much more expensive than the mixed oxide routes. The use of mixed barium titanium oxalates has been very successful in producing high-quality fine-grained barium titanate powder for use in the capacitor industry. The use of metal citrates (frequently called the Pechini process) has been successfully used on a research scale to prepare many different types of ferroelectric oxide, but this type of process has not been applied on a commercial scale. Metal alkoxides, such as titanium isopropoxide, are readily soluble in alcohols and will react quickly with water to precipitate a hydroxide gel. Workers have used mixtures of titanium and zirconium alkoxides with lead and lanthanum acetates to coprecipitate a mixed hydroxide gel that could be calcined and sintered to make transparent lead lanthanum zirconate titanate ceramics for electro-optical applications.

### 26.3.3 Thick Films

There has been considerable interest in the integration of thick (10–50 μm thick) films of ferroelectric materials with alumina and other types of substrates such as silicon, to complement the wide range of other thick-film processes that are available, covering conductors, dielectrics, magnetic materials etc. There are many potential advantages to thick film processing for making certain types of sensor, especially the ability to use screen-printing for depositing the patterns of the materials required. Screen-printing involves using a sheet of wire mesh (the *screen*) that is coated with a photosensitive polymer. Exposure and development of the polymer allows selected areas to be removed, opening regions through which a paste of the required material can be pushed using a rubber blade or squeegee. The principle is simple, but there is a considerable amount of know-how in the formulation of the paste, which consists of the active material (in this case a ferroelectric powder such as PZT), an organic vehicle (a mixture of a solvent and polymer) and a glass frit. The screen is stretched over a former, and held close to, but not in contact with, the surface onto which the print is required. The paste is placed on the screen, and then spread over the screen with the squeegee, which prints the paste onto the substrate. Successive layers of different materials can be printed and cofired, provided there is good compatibility between them. The process has been well developed for piezoelectric films and adequate properties have been obtained from the films, although they are still well below the values that could be expected



from a bulk ceramic material. (See review by *Dorey and Whatmore* [26.28] for further details.)

### 26.3.4 Thin Films

The integration of high-quality thin films ( $< 0.1\text{--}5\ \mu\text{m}$  thick) of ferroelectric materials onto substrates such as silicon has excited considerable interest for potential applications ranging from nonvolatile information storage to their use as active materials in micro-electro-mechanical systems (MEMS), where they can potentially be used for microsensors and actuators. Almost all the interest has been in the use of oxide ferroelectrics, but there has been some interest in the use of P(VDF-TrFE) copolymer films. These can be spun onto electroded substrates from methyl ethyl ketone solution. They are dried at relatively low temperatures ( $< 100^\circ\text{C}$ ) and crystallised by annealing at  $180^\circ\text{C}$  for several hours [26.29]. Such films have been applied to pyroelectric devices. However, the activity coefficients which can be obtained from such films are much lower than those that can be obtained from oxide materials. A range of deposition techniques have been developed for growing ferroelectric oxide films, which are summarised below:

- **Chemical solution deposition (CSD):** This term is applied to a wide range of processes that involve taking the metal ions into metalorganic solution, which is then deposited on the substrate by spinning, followed by drying and annealing processes to remove the volatile and organic components and convert the layer into a crystalline oxide. There are two broad classes of CSD process: metalorganic deposition (MOD) and sol gel. The MOD processes usually involve dissolving metal complexes with long-chain carboxylic acids in relatively heavy solvents such as toluene. The carbon content of the precursors is quite high, so there is a good deal of thickness shrinkage during firing. MOD solutions tend to be quite stable with time and resistant to hydrolysis. Sol-gel processes use precursors such as metal alkoxides, acetates and  $\beta$ -diketonates in alcohol solution. (For example, a set of precursors to deposit PZT would be Ti isopropoxide, Zr n-propoxide and lead acetate). Alkoxide precursors are very susceptible to hydrolysis, and so careful control of moisture content during the sol synthesis is essential and stabilisers such as ethylene glycol are usually added to the solutions to extend the useable lifetimes of the sols. Whereas MOD solutions are true solutions, the sols are actually stable dispersions of metal oxide/organic ligand particles with a size of about 4–6 nm. Sols possess lower viscosi-

ties and tend to produce the oxide layer at a somewhat lower temperature than the MOD processes, but the individual layer thicknesses produced by a single spin tend to be lower. Single crack-free layers tend to be in the range 100–200 nm thick. CSD processes have the advantages that they are low cost, the composition can be easily changed and they produce very smooth layers. The processes are planarising and will not follow underlying surface topology, which can be a disadvantage. Also, the processes are not industry standard in that they are wet and tend to have many variations.

- **Metalorganic chemical vapour deposition (MOCVD):** This is a variation on the process that has been very successfully applied to the growth of group III–V semiconductor layers. The principle is simple: volatile metalorganic compounds are passed over a heated substrate, where they decompose to form a layer of the desired compound. The problem with the growth of ferroelectric oxides is that most of the available metal organic precursors are relatively nonvolatile at room temperature. There has, therefore, been a great deal of research into the available precursors for the compounds that are required. Metal alkyls (such as lead tetraethyl) are very volatile, but only available for relatively few of the metal ions of interest (Pb being the main one). They are also pyrophoric and highly toxic. Some metal alkoxides, such as Ti isopropoxide, are suitable MOCVD precursors. Metal  $\beta$ -diketonates and related compounds such as tetramethyl heptane dionates (THDs) have received considerable attention as Ba and Sr precursors. All of these precursors need to be heated to give them suitable volatility and this means that the lines connecting the precursor source to the growth chamber need to be heated as well. Some of the precursors (especially THDs) are solids, which means that they are not really suitable for use in conventional bubbler-type sources. There has been considerable success in using solutions of these compounds in tetrahydrofuran (THF). The solutions are sprayed into a vaporiser that consists of a cylinder, containing wire wool or ball bearings, heated to a temperature at which the solution will flash-evaporate. A carrier gas is passed through the cylinder and this carries the precursor vapour into the growth chamber. The growth chamber is usually held at reduced pressure and a certain amount of oxygen is introduced to aid the oxide deposition. Frequently a radio-frequency (RF) or microwave plasma is also introduced to aid the growth of a high density film and reduce the required substrate temperature. The major problem

with the MOCVD process for complex ferroelectric oxides which have many cation components is finding the right combination of precursors that will all decompose at the same substrate temperature (usually ca. 550–650 °C) at a rate that will give the desired composition in the film. The process has been very successful in growing thin films of materials such as (Ba,Sr)TiO<sub>3</sub>, with potential applications in the dynamic random-access memory (DRAM). The major advantage of MOCVD is that it is a truly conformal growth technique, with major advantages for semiconductor devices with complex topologies, but is a very expensive technique to set up because of the complex growth and control systems needed. Also, precursor availability is still a problem for many systems.

- **Sputtering:** A range of sputtering processes have been applied to the growth of ferroelectric thin films, including RF magnetron sputtering, direct-current (DC) sputtering and dual ion-beam sputtering. The RF magnetron process is probably the most popular. With all the processes, the major problem is one of obtaining the correct balance of cations in the growing film. Many different solutions have been found to this problem. In reactive sputtering, a composite metal target can be used. This can be made of segments of the metals to be sputtered (for example, Pb, Zr and Ti for PZT) and their relative areas changed to obtain the right composition in the film. Alternatively, multiple targets can be used and the substrate exposed to each one for different lengths of time, or the power applied to each one can be varied. In reactive sputtering, it is necessary to have an amount of oxygen in the sputtering gas (usually Ar). It is possible to sputter ferroelectric thin films from ceramic or mixed powder targets, but it is necessary to adjust the target composition to allow for different yields for each element. In any sputtering process there are many variables to adjust to optimise the process, including the sputtering power, and RF or DC substrate bias, which will affect the ion bombardment of the growing film, the sputtering atmosphere pressure and gas mixture and the substrate temperature. All of these can affect the film growth rate, composition, crystallite size and crystalline phases that are deposited, and the stress in the growing film. For this reason, the development of a sputtering process for a complex ferroelectric oxide can be a time-consuming business, and once a set of conditions has been arrived at for one particular composition, it cannot quickly be changed to accommodate new compositions. Dual ion-beam sputtering differs from the RF and DC processes in that a much lower back-

ground pressure is used, the material is sputtered from the target using an ion beam and a second lower-energy ion beam is used to stimulate and densify the growing film. The sputtering processes have the advantage of being well accepted industrially, as they are dry and can readily coat large-area substrates.

- **Laser ablation:** This process involves bombarding a ceramic target with a pulsed, focussed laser beam, usually from an ArF excimer source. The target is held under vacuum. A plasma plume is produced and the products ablated from the target are allowed to fall on a heated substrate. The advantages of the process are that there is usually good correspondence between the composition of the target and the growing film. Relatively small ceramic targets are acceptable for the process, and it is thus a good method for getting a rapid assessment of the properties of thin films of a given material. The disadvantages of the process are that the plasma plume will only coat a relatively small area of substrate, although there are now systems which use substrate translation to coat large areas, and particles can be ablated from the target, causing defects in the growing film.

In all the techniques used for the growth of ferroelectric oxide thin films, the key issues are control of composition and the formation of the desired crystalline phase (usually perovskite) with the desired crystallinity (crystallite size, morphology and orientation). All of the ferroelectric perovskites have a tendency to crystallise into a non-ferroelectric fluorite-like pyrochlore phase at low temperatures. In the case of the CSD processes, this means that as the film is heated from room temperature, after it loses the organic components, it first forms an amorphous oxide which then crystallises into a nanocrystalline pyrochlore phase, finally forming the desired perovskite phase. The temperatures at which this will occur depend very much on the ferroelectric oxide that is being grown and the precise composition. In the case of PZT, the pyrochlore phase will form above about 300–350 °C. The perovskite phase will start to form above about 420 °C, depending upon the ratio of Zr : Ti in the solid solution. The compositions close to PbTiO<sub>3</sub> will crystallise into perovskite much more readily than those close to PbZrO<sub>3</sub>. In the case of a complex perovskite, such as Pb(Mg<sub>1/3</sub>Nb<sub>2/3</sub>)O<sub>3</sub> or PbSc<sub>1/2</sub>Ta<sub>1/2</sub>O<sub>3</sub>, the pyrochlore phase is much more stable and much higher temperatures (> 550 °C) are needed to convert it to perovskite. Excesses of PbO will tend to favour the formation of perovskite, and deficiencies favour pyrochlore. Higher annealing temperatures will promote PbO loss and it is

possible to get into a position, through PbO loss, where the pyrochlore becomes the most stable phase, even at high annealing temperatures. Residual pyrochlore phase invariably compromises the electrical properties of the films through reduced permittivity and piezoelectric/pyroelectric coefficients. The other growth techniques have the advantage that the films can be deposited onto heated substrates, at temperatures where they will grow directly into the perovskite phase (at least in principle), although there are many examples in the literature of films being deposited (e.g., by sputtering) at low substrate temperatures and converted to the desired perovskite phase by post-deposition annealing, in which case the same problems of pyrochlore formation apply. The control of film crystallinity (crystallite orientation and size) is important as it has a direct effect on the electrical properties. This is usually achieved through control of the crystallite nucleation. Sputtered Pt is frequently used as a substrate onto which ferro-

electric thin films are grown. Like many metals, this will naturally grow with a (111) preferred orientation. It is face-centred cubic (fcc), with a lattice parameter of about  $3.92 \text{ \AA}$ , which matches the lattice parameters of many of the ferroelectric perovskites, which are about  $4 \text{ \AA}$ . This means that, with appropriate process control, it is quite possible to get a highly orientated (111) ferroelectric film on Pt, with a crystallite size of about 100 nm. Changing the underlying nucleation layer can allow other orientations to be grown. For example, the use of thin films of  $\text{TiO}_2$  or PbO on top of the Pt electrode can induce a (100) orientation. It is important to control the nucleation density of the perovskite phase. If this is allowed to become too low, than large circular grains several microns in diameter (called *rosettes*) can form, which tend to induce defects at their boundaries. (Further details on thin-film ferroelectric growth techniques can be found in the book by *Pas de Araujo* et al. [26.30]).

## 26.4 Ferroelectric Applications

### 26.4.1 Dielectrics

As noted above,  $\text{BaTiO}_3$  possesses a very high permittivity close to  $T_C$ . The inclusion of selected dopants can reduce  $T_C$  and optimise the properties of the material for capacitor applications. The substitution of  $\text{Sr}^{2+}$  for  $\text{Ba}^{2+}$ , for example, will reduce it, so that at about 15% substitution it will occur at about  $20^\circ\text{C}$ . Substitution of  $\text{Zr}^{4+}$  for  $\text{Ti}^{4+}$  has a similar effect. The use of off-valent substitutions will have an effect upon resistivity and degradation characteristics, so that substituting  $\text{La}^{3+}$  on the A site will reduce resistivity at low concentrations. Substituting  $\text{Nb}^{5+}$  on the B site at the 5% level has been shown to confer resistance to degradation. The addition of Mn to the lattice has been shown to have a positive effect on dielectric loss. Control of grain size has also been shown to have a marked effect on dielectric properties. Reducing the grain size has the effect of increasing the concentration of domain walls per unit volume of ceramic, and thus increasing the domain-wall contribution to the permittivity. A reduction in grain size also brings about an increase in the unrelieved stress on the grains, which further increases the permittivity. Once the grain size falls below about  $0.5 \mu\text{m}$ , the stress on the grains reduces their tetragonality and the permittivity falls. It is also possible to use heterogeneity in the ceramic grains to flatten the curve of dielectric constant versus temperature. A range of Electronic Industries Alliance (EIA) codes have been introduced to define the variation of capacitance with

temperature. The X7 temperature range, for example, is  $-55$  to  $+125^\circ\text{C}$ , while following this with the letter R would specify a capacitance change of no more than  $\pm 15\%$ . Other dielectrics have been developed based on PMN that have higher peak permittivities, but worse temperature characteristics, capable of meeting a Z5U specification ( $+22$  to  $-56\%$  capacitance variation over the range of  $10$ – $85^\circ\text{C}$ ) but not much better. There has been huge progress in MLC technology, with capacitors now available with  $> 100$  layers of submicron thickness and capacitances ranging from a few hundred pF to  $100 \mu\text{F}$ . The majority of these now have base-metal (Ni) electrodes. The fabrication of the ceramic dielectrics for these is a very complex area and a great deal of technology has been developed to service a very large MLC capacitor market (615 Bn units in 2002, worth an estimated  $\$ 8.4$  Bn).

### 26.4.2 Computer Memories

The storage of digital information is of great interest and growing technological importance. The ability of ferroelectrics to store information via the sense of the spontaneous polarisation has made them candidates for this application ever since the advent of the electronic computer. However, it is only with the development of the techniques for the growth of ferroelectric thin films onto silicon at relatively low temperatures (see above) that their use has become a reality. There are two ways in which ferroelectrics can be used in com-

puter memories. The first is the replacement of the dielectric layer in dynamic random-access memories (DRAMs). Here, the motivation is to exploit the high permittivities exhibited by ferroelectric oxides to reduce the area of silicon required to store a single bit of information. The favoured materials here are based on (Ba, Sr)TiO<sub>3</sub>, while the favoured technique for thin-film growth is plasma-enhanced MOCVD because of its ability to deposit conformal coatings. No DRAM devices using these thin films have yet reached the market place. The use of the switchable polarisation for the nonvolatile storage of information has received a great deal of research. A good deal of this work has been based upon the use of PZT thin films, grown by a variety of techniques, including CSD, RF sputtering and MOCVD. Initially, there were many problems to solve, including the decay of the switchable polarisation (ca. 35 μC/cm<sup>2</sup>) as the number of switching cycles increased (fatigue), the tendency for the polarisation in a bit to become less easily switched with time and the number of times it is switched in the same sense (imprint) and the tendency for the switchable polarisation in any one bit to decay with time (retention). The fatigue and imprint problems in PZT have been ascribed to the motion of oxygen vacancies addressed by the use of oxide, rather than metallic, electrodes and doping to reduce the vacancy concentration. It has also been demonstrated that Aurivillius compounds such as strontium bismuth tantalate (SBT) and La-doped Bi<sub>4</sub>Ti<sub>3</sub>O<sub>12</sub> do not show fatigue behaviour, although they do require rather higher growth temperatures than the PZT family and have a significantly smaller switchable polarisation (ca. 7 μC/cm<sup>2</sup>). A number of companies are now making chips with nonvolatile on-board embedded ferroelectric random-access memory (FRAM). These are going into applications such as smart cards and computer games.

### 26.4.3 Piezoelectrics

This represents the most diverse range of applications for ferroelectric materials, as noted in the introductory section, covering a wide range of sensors, actuators and acoustic wave components for frequency control and filtering applications. The key properties determining the performance of a piezoelectric material in a particular application are the piezoelectric coefficients, elastic and dielectric constants. These are all tensor properties (see Nye [26.31]) and are combined through the constitutive equations

$$D_i = d_{ijk}X_{jk} + \epsilon_{ij}E_l,$$

$$x_{ij} = s_{ijkl}^E X_{kl} + d_{mij}E_m,$$

where  $D_i$  = electric displacement,  $E_i$  = electric field,  $X_{ij}$  = stress,  $x_{ij}$  = strain,  $d_{ijk}$  = piezoelectric coefficients,  $\epsilon_{ij}^X$  = dielectric permittivity coefficients at constant stress, and  $s_{ijkl}^E$  = elastic compliance coefficients at constant electric field.

The above equations use the Einstein repeated-suffix tensor notation. Note that most piezoelectric equations use the reduced-suffix notation for the piezoelectric and elastic constants [26.31].

There are two basic modes of operation for piezoelectric sensors and actuators. The first is well away from any mechanical resonance – usually at low frequency or quasi-DC. Here, the electric signals generated by an applied stress, or the strain generated by an applied electric field can be easily calculated using the constitutive equations of the type quoted above. The commonly used modes for operating piezoelectric ceramic actuators are longitudinal, where the electric field is applied parallel to the direction in which strain is required and the coupling is via the piezoelectric  $d_{33}$  coefficient, and transverse, where a field is applied along the polar axis, but the exploited strain is perpendicular to this direction and coupling is via the  $d_{31}$  and  $d_{32}$  coefficients. Corresponding modes are frequently used for piezoelectric sensors. The two most-commonly used actuator structures are illustrated in Fig. 26.15. Figure 26.15a shows a piezoelectric bimorph, in which two pieces of piezoelectric ceramic are bonded to a central metal shim. Fields are applied parallel to the polar axes of the ceramic elements so that their transverse extensions are equal and opposite. Usually one end of the bimorph is clamped so that the other end bends. In a variation on this structure, a single piece of ceramic is bonded to a piece of metal, making a unimorph. Bimorph and unimorph devices can provide high displacements (several tens to thousands of microns at up to 200-V drive) but relatively low forces (typically up to 1 N), depending on the size of the bimorph. The second widely used actuator structure is the multilayer

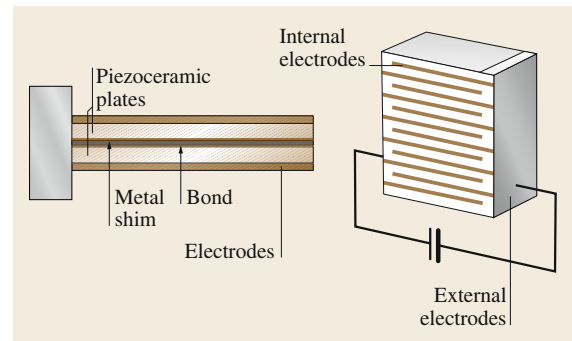


**Fig. 26.15** (a) Piezoelectric bimorph and (b) MLC actuator structures

ceramic actuator (Fig. 26.15b). This device operates in longitudinal mode, with applied field and extension parallel to the polar axis. The division of the structure into many thin layers reduces the voltage required to obtain a given extension. Typical devices can produce a few to a few tens of microns extension at a few hundred Volts (depending on dimensions) but high forces (in the kilo-Newtons range). It is also possible to use a shear mode of operation for both sensing and actuation. In this actuation mode, the field is applied perpendicular to the polar axis and a shear strain is generated in the plane containing the vectors parallel to the applied field and the polar axis.

Many piezoelectric devices are operated under an alternating electric field whose frequency is tuned to match a mechanical resonance. A piezoelectric element operated well away from resonance will exhibit a capacitive impedance characteristic. As a mechanical resonance is approached, the electrical behaviour of the element can be characterised using an equivalent circuit as shown in Fig. 26.16a.  $C_0$  is the static capacitance. The  $L_m$ ,  $R_m$ , and  $C_m$  form the motional arm of the circuit. If the admittance of such a circuit is plotted as a function of frequency, a behaviour is obtained as shown in Fig. 26.16b. The maximum in the admittance is very close to the mechanical resonant frequency ( $f_r$ ), while the minimum in the admittance is close to antiresonance ( $f_a$ );  $f_r$  is determined by the elastic properties of the piezoelectric, its density and the dimensions relevant to the particular resonant mode. It is useful to define an effective electromechanical coupling coefficient  $k_{\text{eff}}$  which is defined by

$$k_{\text{eff}}^2 = \frac{\text{mechanical energy converted to electrical energy}}{\text{input mechanical energy}}$$

or

$$k_{\text{eff}}^2 = \frac{\text{electrical energy converted to mechanical energy}}{\text{input electrical energy}},$$

$k_{\text{eff}}$  can be determined from  $f_r$  and  $f_a$

$$k_{\text{eff}}^2 \approx \frac{f_a^2 - f_r^2}{f_a^2}.$$

It can be shown that, for a simple resonant mode of a piezoelectric element,  $k_{\text{eff}}$  takes the form

$$k_{\text{eff}}^2 = \frac{d^2}{s^E \epsilon^X}$$

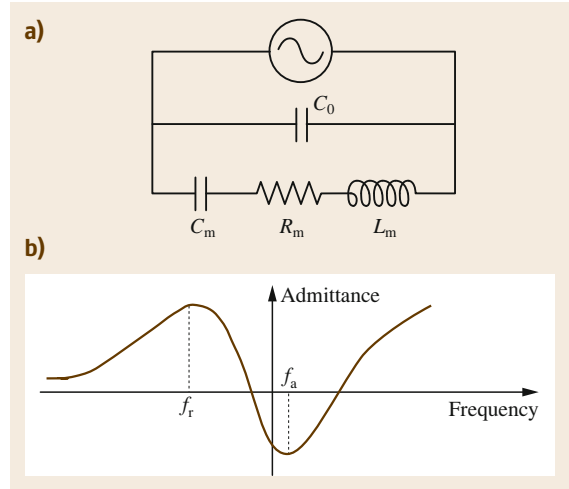


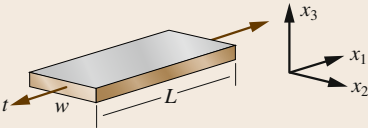
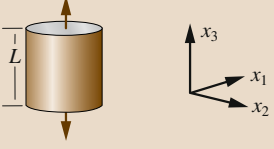
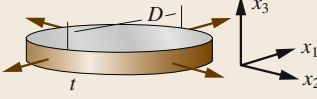
**Fig. 26.16** (a) Piezoelectric element equivalent circuit (b) Admittance versus frequency for a typical piezoelectric resonator

where the  $d$ ,  $s$  and  $\epsilon$  coefficients in this equation are combinations of the piezoelectric, elastic and dielectric permittivity coefficients. The precise combination of the coefficients will depend on the shape of the piezoelectric element and the mode being excited into resonance. A list of the more commonly used modes and the dependence of  $k_{\text{eff}}$  on the relevant materials constants is given in Table 26.4. For more complex structures, such as those which involve a piezoelectric element (or elements) bonded to a metal component, it is still possible to define and measure a  $k_{\text{eff}}$ , but its value will be a much more complex combination of the materials constants, and will also involve the properties of the metal parts and the relative dimensions of the piezoelectric and metal components. (For more details refer to the IEEE standards on piezoelectricity).

By far the most widely exploited piezoelectric materials system is based on the  $\text{PbZr}_x\text{Ti}_{1-x}\text{O}_3$  ceramic solid solution series. Most of the compositions of-interest are centred on the morphotropic phase boundary (MPB) region (Fig. 26.7) with  $x = 0.52$ . In the undoped series, the piezoelectric coefficients and dielectric constants peak at this composition. However, their properties can be greatly enhanced by the inclusion of selected cation dopants. These can be classified as follows:

- **Isovalent:** These are divalent cations that will substitute for  $\text{Pb}^{2+}$  on the A site (e.g.,  $\text{Sr}^{2+}$ ) or tetravalent ions (e.g.,  $\text{Sn}^{4+}$ ) substituting for  $\text{Ti}/\text{Zr}^{4+}$  on the B site.
- **Donors:** These are cations with a valency greater than the site onto which they substitute (e.g.,  $\text{La}^{3+}$  for  $\text{Pb}^{2+}$  or  $\text{Nb}^{5+}$  for  $\text{Ti}/\text{Zr}^{4+}$ ).

**Table 26.4** A list of the most commonly used piezoelectric resonances and the dependence of the  $k_{\text{eff}}$  for each on the piezoelectric, elastic and dielectric constants. (After [26.32])

Mode type	Mode shape	Coupling factor
Length extensional mode of a bar using transverse excitation $L > 5w, L > 10t$		$k_{31}^l = \frac{d_{31}}{\sqrt{\epsilon_{33}^T s_{11}^E}}$
Length extensional mode of a cylindrical rod using longitudinal excitation $L > 10 \times \text{diameter}$		$k_{33}^l = \frac{d_{33}}{\sqrt{\epsilon_{33}^T s_{33}^E}}$
Radial mode of a round plate using longitudinal excitation $D > 20 \times \text{thickness}$		$k_p = \frac{k_{31}}{\sqrt{2/(1-\sigma^p)}}$
Grey areas denote the electroded surfaces		

**Table 26.5** The effects of substituents in the PZT system. (After [26.11])

Isovalent substituents, e.g., $\text{Sr}^{2+}$ for $\text{Pb}^{2+}$ , $\text{Sn}^{4+}$ for $\text{Zr}^{4+}$	Donor substituents, e.g., $\text{La}^{3+}$ for $\text{Pb}^{2+}$ , $\text{Nb}^{5+}$ for $\text{Zr}/\text{Ti}^{4+}$
Lower Curie point	No change in Curie point
Increase permittivity	Higher permittivity
Small improvement in linearity at high drive	Higher electromechanical coupling
No change in coupling factor, aging, volume resistivity or low amplitude mechanical or dielectric loss	Poorer high drive linearity
	Lower aging
	Increase resistivity
	Reduced $Q_E$ and $Q_M$
Acceptor substituents, e.g., $\text{K}^+$ for $\text{Pb}^{2+}$ ; $\text{Fe}^{3+}$ for $\text{Zr}/\text{Ti}^{4+}$	Variable valence substituents, e.g., Mn – can be 2+, 3+, 4+ – for $\text{Zr}^{4+}$
No change in Curie point	No change in Curie point
Lower permittivity	Range of permittivity
Lower electromechanical coupling	Range of electromechanical coupling – usually lower
Improved drive linearity	High drive/linearity not changed
Little change in aging	Reduced aging
Volume resistivity reduced	
Increased $Q_E$ and $Q_M$	

- Acceptors: These are cations with a valency lower than the site onto which they substitute (e.g.,  $\text{K}^+$  for  $\text{Pb}^{2+}$  or  $\text{Ni}^{3+}$  for  $\text{Ti}/\text{Zr}^{4+}$ ).
- Multivalent: These are ions that take multiple valency (e.g., Mn substituted on the B site).

The broad effects of each class of dopants are listed in Table 26.5.

The resulting PZT ceramics are broadly classified into *hard* or *soft* according to whether they are doped with acceptors or donors, respectively. Each manufacturer has its own nomenclature scheme for its piezoe-

ramic products. However, the US Navy produced a set of specifications under MIL-STD-1376B which are universally recognised. Hard ceramics (e.g., US Navy type III) have relative permittivities in the range of 1000 with high  $Q_s$  ( $> 500$ ) and  $d_{33}$  of about 215 pC/N. Soft ceramics (e.g., US Navy type VI) have much higher permittivities (3250) and piezoelectric coefficients ( $d_{33} = 575$  pC/N) but lower  $Q$ 's (65). Hard ceramics have much better drive-voltage stability and higher Curie temperatures than soft ceramics. The soft compositions tend to be used for actuator applications, where the maximum piezoelectric displacement for a given drive

**Table 26.6** Typical values for the piezoelectric, dielectric and elastic properties of some selected piezoelectric ceramic materials. (Taken from [26.33])

Material type	I	III	V	VI	Units
Stress-free relative permittivity ( $\epsilon_{33}$ )	1275	1025	2500	3250	
Dielectric loss tangent ( $\tan \delta$ )	$\leq 0.006$	$\leq 0.004$	$\leq 0.025$	$\leq 0.025$	
$d_{33}$	290	215	495	575	pC/N
$k_p$	0.58	0.50	0.63	0.64	
Mechanical quality factor $Q_m$	$\geq 500$	$\geq 800$	$\geq 70$	$\geq 65$	
Curie temperature ( $T_C$ )	325	325	240	180	$^{\circ}\text{C}$

voltage is sought, while soft ceramics tend to be used for resonant and sound-generation applications. There are, however, exceptions to this. Medical ultrasound transducer arrays tend to use soft, high-permittivity ceramics, because they need to have the maximum charge sensitivity in the reception of the sound waves reflected from tissues within the body, and high permittivities because the small elements usually need to drive transmission lines with significant capacitance.

There are other types of piezoelectric ceramics that are used for specialist applications. Modified  $\text{PbTiO}_3$  ceramics possess very low values of  $d_{31}$  and tend to be used for ultrasound array applications where small cross-coupling between adjacent elements is important. They also possess much higher response to hydrostatic stress than MPB PZT ceramics. Because of this, arrays of small blocks of this type of ceramic are used in flank array sensors in submarines. As noted above, lead metaniobate ceramics are used in high-temperature applications. Table 26.6 lists the piezoelectric and other properties of some selected piezoelectric ceramics.

Single crystals of PZN-PT and PMN-PT have received considerable attention because of the very high piezoelectric  $d_{33}$  coefficients and  $k_{33}$  coupling factors that can be obtained and single-crystal plates of these are now commercially available. Table 26.7 lists some of the properties that have been measured from these materials, and compares them with a commercial soft PZT ceramic.

Single crystals of  $\text{LiNbO}_3$  are widely used in surface acoustic wave devices. In these, interdigitated

**Table 26.7** Piezoelectric properties of PMN-PT single crystal materials [26.34] compared with those of a commercial soft-piezoelectric ceramic HD3203 [26.35]

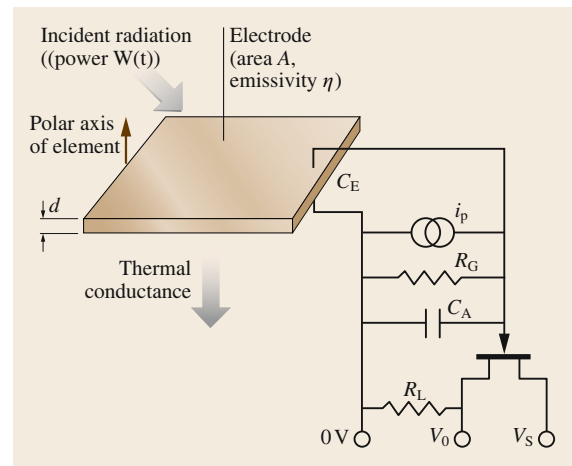
Property	Composition	
	PMN-PT X2B	HD3203
$\epsilon_{33}^T/\epsilon_0$	5000–7500	3370
$T_{RT}$ ( $^{\circ}\text{C}$ )	85–98	NA
$T_C$ ( $^{\circ}\text{C}$ )	$> 142$	195
$k_t$ (%)	55–59	0.536
$k_{33}$ (%)	91–95	0.763
$N_{33}$ (Hz.m)	599	2000
$d_{33}$ (pC/N)	1500–2300	564

electrodes (IDEs) are applied to one polished face of a crystal. Excitation of these with an RF field will cause the generation of piezoelectrically excited Rayleigh waves, which will propagate with very little attenuation. These can be detected by further sets of IDE placed on the same face of the crystal. Such devices are widely used in signal processing and filtering applications in mobile telecommunication applications.

Thin films of piezoelectric materials, excited into thickness-mode resonance, are being explored for very-high-frequency ( $> 1$  GHz) resonant filter applications. Thin films of PZT are now widely used in inkjet printers.

#### 26.4.4 Pyroelectrics

The pyroelectric effect is now widely used in uncooled detectors of long-wavelength infrared radiation (IR). The principle behind the operation of these devices is very simple. The radiation to be detected is allowed to fall upon a thin chip of the pyroelectric material. The energy absorbed causes a change in temperature and the generation of a pyroelectric charge, which will cause the flow of current in an external circuit. This can be amplified and used, for example, to switch an alarm. The basic circuit of a pyroelectric detector is shown


**Fig. 26.17** Schematic diagram of a pyroelectric IR sensor

schematically in Fig. 26.17. The field-effect transistor (FET) amplifier needs to be close to the pyroelectric element, ideally in the same package. This is because the latter has a very high output impedance and thus is very noise sensitive. The pyroelectric signal is represented in this circuit as a current source,  $i_p$ .  $i_p$  is proportional to the rate of change of the element temperature with time. Pyroelectric devices do not have a DC response. They only see changes in the intensity of the radiation with time. This is a major advantage in many applications, where usually there is a requirement to detect changes in the radiation coming from a scene, rather than the average or unchanging background intensity. An example of this is the requirement to detect the radiation from a person coming into the field of view of an IR detector.

Pyroelectric devices have several advantages over other radiation detectors. Their response is independent of the wavelength of the incident radiation, provided there is some means to absorb the radiation. Hence, pyroelectric radiation detectors have been used across the full range of the electromagnetic spectrum, from microwaves to x-rays. Basically a single pyroelectric detector design can be used for different wavelengths of radiation, simply by equipping the package with different windows coated with filters according to the radiation it is desired to sense. Such devices are widely used in spectroscopic sensors for, e.g., automotive exhaust-gas analysis. However, by far the widest application of pyroelectric detectors is in the sensing of IR in the wavelength range 8–14  $\mu\text{m}$ . The reasons for this are that there is an atmospheric window of low absorption and that objects with temperatures in the range of room temperature (300 K) emit most of their radiative energy in that waveband. However, all of the semiconductor detectors of 8–14  $\mu\text{m}$  IR need to be cooled to about 77 K to work efficiently. On the other hand, pyroelectric detectors work perfectly well uncooled. Cheap detectors are readily available for under \$1, and have thus found their way into a host of applications, notably detectors of people in such things as intruder alarms and remote light switches. Pyroelectric arrays have been developed in which a plane of pyroelectric material is interfaced to a silicon chip bearing a two-dimensional array of FET amplifiers and a set of switches which can be used to multiplex the pyroelectric signals onto a single output. These arrays have been used for uncooled thermal imagers with performances comparable to those that can be achieved with cooled semiconductor devices [26.36].

The requirements for the active materials in a pyroelectric device has been described by, for example, *Whatmore* [26.22], *Whatmore and Watton* [26.36]. There are two time constants that determine the frequency response of a pyroelectric device: the elec-

trical time constant determined by  $R_G(C_E + C_A)$  (see Fig. 26.17) and the thermal time constant determined by  $H/G$  where  $H$  is the heat capacity of the pyroelectric element and  $G$  the thermal conductance from the pyroelectric element to the environment. The capacitance of the element ( $C_E$ ) is determined by the permittivity ( $\epsilon$ ) of the pyroelectric material while the heat capacity is determined by its specific heat per unit volume ( $c'$ ). The pyroelectric current is proportional to the material's pyroelectric coefficient ( $p = dP_s/dT$ ). A full treatment of the physics of device operation shows that detector performance (as determined by specific detectivity) is proportional to one of three basic figures-of-merit (FOMs), which combine the pyroelectric, dielectric and thermal properties of the pyroelectric material together. If the pyroelectric element capacitance is small in comparison with the amplifier capacitance ( $C_A$ ), then the appropriate FOM is  $F_I = p/c'$ . If  $C_E \gg C_A$  and the noise in the device is dominated by the amplifier noise sources, then the appropriate FOM is  $F_V = p/c'\epsilon$ . If the noise is dominated by alternating-current (AC) Johnson noise in the pyroelectric element then the appropriate FOM is  $F_D = p/c'\sqrt{\epsilon \tan \delta}$ , where  $\tan \delta$  is the dielectric loss tangent of the pyroelectric material. Note that it is very important to measure the dielectric constant and loss at a frequency relevant to the device use. As most pyroelectric devices are used in the frequency range 0.1–100 Hz, and dielectric loss is usually much greater at < 100 Hz than at 1 kHz, a low-frequency measurement is essential. Table 26.8 lists the pyroelectric properties of several ferroelectric materials. Note that many of the literature papers on the subject only quote 1 kHz dielectric measurements. The differences between the FOM for the materials where high- and low-frequency data are available are clear. It can be seen that that the DTGS (deuterated triglycerine sulfate) family gives the largest figures of merit. However, these materials are water soluble and have relatively low Curie temperatures and so they are only still used in the high-performance devices for instruments such as in Fourier-transform infra-red (FTIR) spectrometers. LiTaO<sub>3</sub> (LT) is a good pyroelectric material with relatively low permittivity. It is inert and relatively easy to handle. It is used in many single-element detectors. Ceramic materials such as those based on modified PbZrO<sub>3</sub> (Mod PZ) or modified PbTiO<sub>3</sub> (Mod PT) are widely used in low-cost detectors. Note that, although their FOM are worse than LT, they are low cost and their performance is perfectly adequate for many applications. The PVDF family (represented here by a P(VDF/TrFE70/30 copolymer) have good  $F_V$ , but relatively low  $F_D$  values compared with the other materials listed. They tend to be used in large-area detectors because of their low permittivi-



**Table 26.8** Pyroelectric properties of several ferroelectric materials (taken from *Whatmore and Watton* [26.36])

Material	Meas. $T$ (°C)	$p$ ( $10^{-4} \text{ C m}^{-2} \text{ K}^{-1}$ )	Dielectric properties		Freq. (Hz)	$c'$ ( $10^6 \text{ J m}^{-3} \text{ K}^{-1}$ )	$T_C$ (°C)	$F_V$ ( $\text{m}^2 \text{ C}^{-1}$ )	$F_D$ ( $10^{-5} \text{ Pa}^{-1/2}$ )
			( $\epsilon$ )	( $\tan \delta$ )					
DTGS (Crystal)	40	5.5	43	0.02	1000	2.6	61	0.53	8.3
LiTaO <sub>3</sub> (Crystal)	25	2.3	47	$10^{-3}$	1000	3.2	665	0.17	11.1
P(VDF/TrFE) 70/30 (Polymer)	25	0.33	7.4	0.017	1000	2.3	121	0.22	1.4
Mod. PZ (Ceramic)	25	4.0	290 300	0.003 0.014	1000 33	2.8	230	0.054 0.054	5.2 2.3
Mod. PT (Ceramic)	25	3.5	220 220	0.01 0.03	1000 33	2.8	> 250	0.063 0.063	2.9 1.6

ties, low cost and the fact that they are readily made in very thin films with low thermal mass, which is an advantage in some circumstances. They have been demonstrated in linear arrays. It is advantageous for very small-area detectors (say  $< 100 \mu\text{m}$  square), such as those used in arrays, for the pyroelectric material to have a relatively high permittivity (a few hundred) so that the detector can have a capacitance that matches the input capacitance of the FET amplifier (usually ca. 1 pF). The ceramic materials are well suited to this application for that reason. There has been considerable research into the use in thermal imaging arrays

of ferroelectrics with  $T_C$  close to room temperature under an applied bias field, which will provide an induced pyroelectric effect well above the normal  $T_C$ . This has been called dielectric bolometer mode of operation and the best materials researched for this have been  $\text{Pb}(\text{Sc}_{0.5}\text{Ta}_{0.5})\text{O}_3$  (PST) and  $(\text{Ba}_x\text{Sr}_{1-x})\text{TiO}_3$  solid solutions with  $x \approx 0.35$ . These materials have relative permittivities of  $> 1000$  under the operational conditions and very high pyroelectric coefficients which can give an effective  $F_D$  some three times greater than can be achieved using conventional pyroelectric ceramics [26.37].

## References

- 26.1 G. Busch: *Ferroelectrics* **74**, 267 (1987)
- 26.2 A.F. Devonshire: *Phil. Mag.* **40**, 1040 (1949)
- 26.3 M.E. Lines, A.M. Glass: *Principles and Applications of Ferroelectric Materials* (Clarendon, Oxford 1977)
- 26.4 V.M. Goldschmidt: *Geochemistry* (Oxford Univ. Press, Oxford 1958)
- 26.5 R.D. Shannon, C.T. Prewitt: *Acta Cryst. B* **25**, 925 (1969)
- 26.6 A.M. Glazer: *Acta Cryst. B* **28**, 3384 (1972)
- 26.7 W.J. Merz: *Phys. Rev.* **76**, 1221 (1949)
- 26.8 J.M. Herbert: *Ceramic Dielectrics and Capacitors* (Gordon Breach, Philadelphia 1985)
- 26.9 R.W. Whatmore, A.M. Glazer: *J. Phys. C* **12**, 1505 (1979)
- 26.10 B. Noheda, J.A. Gonzalo, A.C. Caballero, C. Moure, D.E. Cox, G. Sirane: *Ferroelectrics* **237**, 541 (2000)
- 26.11 B. Jaffe, W.R. Cook Jr., H. Jaffe: *Piezoelectric Ceramics* (Academic, New York 1971)
- 26.12 R.W. Whatmore: *Structural Phase Transitions in Modified Lead Zirconate*, Ph.D. Thesis (Cambridge Univ., Cambridge 1977)
- 26.13 G.A. Smolenskii, V.A. Isupov, A.A. Agranovskaya, S.N. Popov: *Fiz. Tverd. Tela* **2**, 2906 (1960)
- 26.14 N.-H. Chan, D.M. Smyth: *J. Am. Ceram. Soc.* **67**, 285 (1984)
- 26.15 N.-H. Chan, R.K. Sharma, D.M. Smyth: *J. Am. Ceram. Soc.* **65**, 168 (1981)
- 26.16 S.C. Abrahams, E. Buehler, W.C. Hamilton, S.J. Laplaca: *J. Phys. Chem. Solids* **34**, 521 (1973)
- 26.17 P.B. Jamieson, S.C. Abrahams, J.L. Bernstein: *J. Chem. Phys.* **48**, 5048 (1968)
- 26.18 L. Keeney, T. Maity, M. Schmidt, A. Amann, N. Deepak, N. Petkov, S. Roy, M.E. Pemble, R.W. Whatmore: *J. Am. Ceram. Soc.* **96**, 2339 (2013)
- 26.19 M.E. Hagerman, K.R. Poeppelmeier: *Chem. Mater.* **7**, 602 (1995)
- 26.20 Y.J. Ding, X.D. Mu, X.H. Gu: *J. Non-Lin. Opt. Phys. Mater.* **9**, 21 (2000)
- 26.21 D. Madgy, S.F. Ahsan, D. Kest, I. Stein: *Arch. Otolaryng. Head Neck Surg.* **127**, 47 (2001)
- 26.22 R.W. Whatmore: *Rep. Prog. Phys.* **49**, 1335 (1986)
- 26.23 H. Kawai: *Jpn. J. Appl. Phys.* **8**, 967 (1969)
- 26.24 J.G. Bergman, J.H. McFee, G.R. Crane: *Appl. Phys. Lett.* **18**, 203 (1971)
- 26.25 J.A. Ghambaryan, R. Guo, R.K. Hovsepian, A.R. Poghosyan, E.S. Vardanyan, V.G. Lazaryan: *J. Optoelectron. Adv. Mater.* **5**, 61 (2003)
- 26.26 R. Clarke, R.W. Whatmore: *J. Cryst. Growth* **33**, 29 (1976)
- 26.27 A. Dabkowski, H.A. Dabkowska, J.E. Greedan, W. Ren, B.K. Mukherjee: *J. Cryst. Growth* **265**, 204 (2004)
- 26.28 R.A. Dorey, R.W. Whatmore: *J. Electroceram.* **12**, 19 (2004)

- 26.29 N. Neuman, R. Köhler: Proc. SPIE **2021**, 35 (1993)
- 26.30 C. Pas de Araujo, J.F. Scott, G.W. Taylor: *Ferroelectric Thin Films: Synthesis and Basic Properties* (Gordon, Breach, Princeton 1996)
- 26.31 J.F. Nye: *Physical Properties of Crystals, Their Representation by Tensors and Matrices* (Oxford Univ. Press, Oxford 1957)
- 26.32 ANSI/IEEE Standard on Piezoelectricity: IEEE Trans. **UFFC 43**, 717 (1996)
- 26.33 MIL-STD-1376B(SH) (1995) US Navy Military Standard for Piezoelectric Ceramics
- 26.34 <http://www.trstechnologies.com/Materials/High-Performance-PMN-PT-Piezoelectric-Single-Crystal>
- 26.35 S. Sherrit, H.D. Wiederick, B.K. Mukherjee: Proc. SPIE **3037**, 158 (1997)
- 26.36 R.W. Whatmore, R. Watton: Pyroelectric Materials and Devices. In: *Infrared Detectors and Emitters: Materials and Devices*, ed. by P. Capper, C.T. Elliott (Chapman Hall, New York 2000) p. 99
- 26.37 R.W. Whatmore, P.C. Osbond, N.M. Shorrocks: *Ferroelectrics* **76**, 351 (1987)